

Cruise Report: R/V *Armstrong* 27 September – 21 October 2022

The Arctic Observing Network: Renewing Observations at the Davis Strait Gateway

by Craig Lee¹, Eric Boget¹, Chris Archer¹, Jed Lenetsky², Kate Stafford³, Angela Szescioraka³,
Kumiko Azetsu-Scott⁴, Carrie-Ellen Gabriel⁴, Maddison Proudfoot⁴, Thomas Juul Pedersen⁵,
Else Ostermann⁵, Tobias Vonnahme⁵, Hannah Felicitas Kuhn⁵, Caroline Gjelstrup⁶,
Bodil Toftegård⁶, Pete Brown⁷, Alice Marzocchi⁷, Lisa Gerlinde Thekla Leist⁸,
Victoria Silverman⁹, Holly Hogan¹⁰, and Siobhan McDonald

¹ *Applied Physics Laboratory, University of Washington*

² *University of Colorado Boulder*

³ *Oregon State University*

⁴ *Bedford Institute of Oceanography*

⁵ *Greenland Institute of Natural Resources and Greenland Climate Center*

⁶ *Danish Technical University*

⁷ *National Oceanography Centre, Southampton*

⁸ *Swiss Federal Institute of Technology*

⁹ *Louisiana Universities Marine Consortium*

¹⁰ *Canada Wildlife Service*

Technical Report
APL-UW TR 2305
September 2023



Applied Physics Laboratory University of Washington
1013 NE 40th Street Seattle, Washington 98105-6698

Acknowledgments

We thank Captain Sheasly and the crew of R/V *Neil Armstrong* for their skill and good-humored support. The Davis Strait Observing System is supported by the U.S. National Science Foundation, Department of Fisheries and Oceans Canada, and the Greenland Institute of Natural Resources.

ABSTRACT

Oceanic freshwater and heat exchange between the Arctic and North Atlantic provide critical mechanisms through which the Arctic and global climate interact. Arctic fresh water, from riverine input and melting sea ice, flows southward through the Arctic Gateways to the west (Davis Strait) and east (Fram Strait) of Greenland into the regions of the subpolar North Atlantic where the waters that occupy the deep ocean interior are formed. At these sites, strong wintertime storms cool the upper ocean, making these waters dense enough to cause them to sink to depth, effectively communicating this atmospheric forcing into the ocean interior and driving the equator-to-pole transport of heat. Fresh, buoyant Arctic outflow reduces the density of surface waters in these deepwater formation regions, and thus has the potential to slow the sinking and modulate equator-to-pole heat transport. Changes in Arctic outflow also impact broad North Atlantic circulation patterns and circulation off the Labrador coast, with wide-ranging impacts to ecosystems. Conversely, the northward flow of relatively warm Atlantic waters can supply oceanic heat to melt Greenlandic glaciers where they encounter the ocean, thus accelerating the melting of Greenland ice cap. Uncertainty surrounding the role of oceanic heat in accelerating the melt of Greenland's glaciers is one of the largest sources of uncertainty in numerical predictions of future sea level rise. The critical role of Arctic-subpolar heat and freshwater exchange motivates renewed efforts to maintain sustained, persistent, measurements across Davis Strait, capturing exchange between the Arctic and subpolar North Atlantic (Labrador Sea) at a choke point at the southern end of Baffin Bay.

This project renews the integrated observational program at Davis Strait, delivering data to the community and matching ongoing collections at Bering Strait, Utqiagvik, Alaska, and Fram Strait to extend the time series of concurrent measurements across the major Arctic Gateways. The extended timeseries will document changes in freshwater and heat fluxes, and will be combined with numerical modeling to investigate the processes that control variability in the strait and the potential impacts. The backbone system relies on the tested combination of moorings instrumented with sensors to measure ice thickness and motion, ocean currents, temperature and salinity, and biennial ship-based sampling of chemical and biological properties that have successfully delivered core measurements for the past decade. Bottom pressure sensors augment the system to quantify sea surface height gradients, which will support investigations of the primary forcing mechanisms. Integrated marine ecosystem observing includes biogeochemical and marine mammal passive acoustic measurements augmented with tracking of key fish species, and zooplankton and phytoplankton observations. These observations will launch the Davis Strait/Baffin Bay Distributed Biological Observatory (DBO) in Davis Strait, complementing the developing Atlantic DBO that includes transect lines in Fram Strait and Barents Sea, and the existing Pacific DBO in the northern Bering, Chukchi, and Beaufort seas.

TABLE OF CONTENTS

1.	Science Background.....	1
2.	Davis Strait Arctic Gateway Observing System	3
3.	Mooring Operations	5
4.	Hydrographic Sampling	23
5.	Underway Surface Water pCO ₂ and TSG	40
6.	Phytoplankton and Particulate Carbon.....	40
7.	Zooplankton	40
8.	Seabirds.....	41
9.	Preliminary Results	41
	Hydrographic Sections.....	41
	Dissolved Organic Matter (DOM)	45
	¹²⁹ I, ²³⁶ U and ¹⁴ C as Transient Tracers of Ocean Circulation.....	46
	Carbonate system/methane/nutrients/dissolved oxygen/oxygen isotope composition (δ ¹⁸ O-H ₂ O)/salinity/CTD/underway pCO ₂ /underway TSG	47
	Total Dissolved Inorganic Carbon (DIC) and Total Alkalinity (TA)	47
	Spectrophotometric pH	47
	Discrete pCO ₂ and Methane	48
	δ ¹⁸ O-H ₂ O	48
	Dissolved Oxygen.....	49
	Salinity	49
	Nutrients.....	49
	Underway Surface pCO ₂	49
	Shipboard Conditions and Problems.....	51
	Phytoplankton and Particulate Carbon.....	52
	Zooplankton Biomass and Vertical Distribution	54
	Seabirds.....	58
	Autonomous and In Situ Water Sampling	63
10.	References.....	69
11.	Appendix: Cruise Narrative	72
12.	Appendix: List of Cruise Participants.....	78
13.	Appendix: Code of Conduct	79

This page is blank intentionally.

1. SCIENCE BACKGROUND

The Arctic freshwater cycle is a longstanding framework for efforts to quantify and understand Arctic change due to its important role in modulating the Arctic energy balance and, further afield, global climate (e.g. *Prowse et al.*, 2015; *Carmack et al.*, 2016). Freshwater enters the Arctic upper ocean primarily through river discharge, Bering Strait inflow and net precipitation, with the majority exiting about equally through the Canadian Arctic Archipelago (CAA) and Fram Strait (*Serreze et al.*, 2006; *Haine et al.*, 2015). Because salinity controls Arctic Ocean stratification, this freshwater creates a cold, buoyant layer below the ice-ocean interface that insulates the surface from the warmer, more saline Atlantic waters below, thus modulating sea ice formation and melt and, through this, coupling between the upper ocean and local atmospheric forcing. Freshwater and heat exchange between the Arctic and North Atlantic provide critical mechanisms through which the Arctic and global climate interact. Arctic freshwater discharges through Davis and Fram straits near deepwater formation regions west and east of Greenland, where its buoyancy may act to modulate convective overturning and deepwater formation (e.g., *Karcher et al.*, 2005; *Jahn and Holland*, 2013, *Yang et al.*, 2016). Changes in Arctic freshwater outflow also modulate the extent and strength of the North Atlantic subpolar gyre, which can have profound impacts on fisheries (*Hatun et al.*, 2009), nutrient flux (*Hatun et al.*, 2017) and on carbon uptake and storage (*Schuster and Watson*, 2007) in this highly productive region. Additionally, northward penetration of warm Atlantic waters along the Greenland coast may accelerate the melting of marine terminating glaciers (e.g., *Holland et al.*, 2008; *Straneo and Heimbach*, 2013; *Myers and Ribergaard*, 2013; *Gladish et al.*, 2015), injecting additional fresh water into the system and contributing to sea level rise.

Davis Strait (**Fig. 1**) provides a single site for quantifying both CAA outflow and northward fluxes along the West Greenland slope and shelf that may impact land ice melt. The CAA component of Arctic outflow enters Baffin Bay through four distinct passages (Bellot Strait, Barrow Strait, Hell Gate/Cardigan Strait, and Nares Strait), undergoing numerous transformations along its transit to Davis Strait. By the time they reach Davis Strait, Arctic waters already embody most of the transformation they undergo prior to exerting their influence on the deepwater formation sites in the Labrador Sea. This makes the Strait an ideal site to quantify the variability and structure of the integrated CAA freshwater flux after it has undergone these complex transformations (*Azetsu-Scott et al.*, 2012), and just prior to entering the Labrador Sea. Sustained observations at Davis Strait also provide early detection of corrosive Arctic outflow into the subpolar North Atlantic, where it may impact highly productive regions and important commercial fisheries; observations document changes in these chemical states and the marine ecosystem response to ocean acidification (*Azetsu-Scott et al.*, 2010; *Hammill et al.*, 2018).

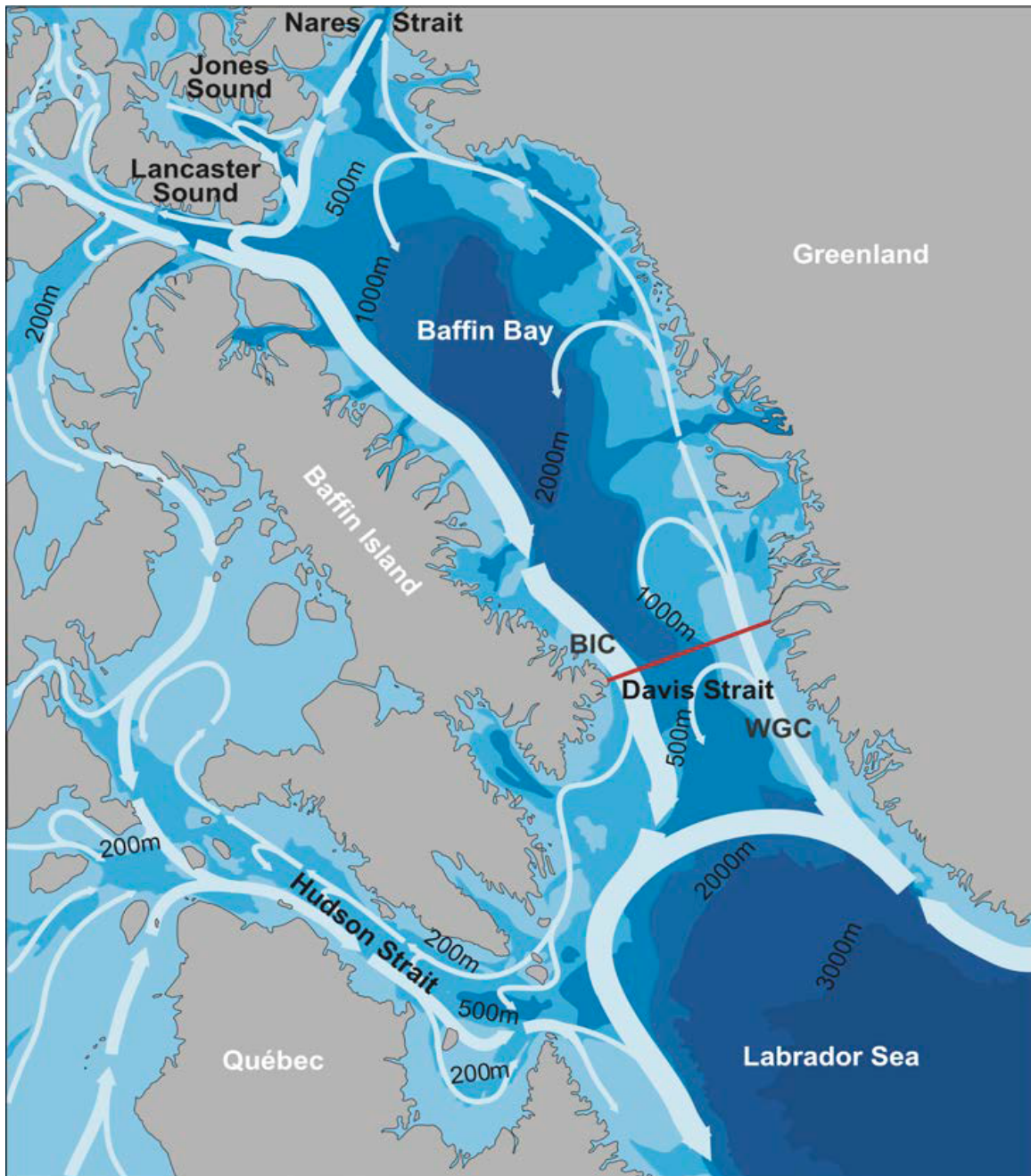


Figure 1. General circulation in Baffin Bay and Davis Strait (white arrows) and the location of the Davis Strait moored array (red line). AW, by way of the CAA, leaves Davis Strait as the broad, surface-intensified BIC. Northward flow on the eastern side of Davis Strait consists of the fresh WGC of Arctic origin on the shelf and warm, salty WGSC of North Atlantic origin on the slope. From Curry et al. (2014).

2. DAVIS STRAIT ARCTIC GATEWAY OBSERVING SYSTEM

The Davis Strait observing system was established in 2004 to advance understanding of the role of Arctic – sub-Arctic interactions in the climate system by collecting sustained measurements of physical, chemical, and biological variability at one of the primary gateways that connect the Arctic and subpolar oceans. Efforts began as a collaboration between researchers at the University of Washington’s Applied Physics Laboratory and Department of Fisheries and Oceans, Canada at Bedford Institute of Oceanography, but has grown to include researchers from the Greenland Institute of Natural Resources, Greenland Climate Institute, Technical University of Denmark, National Oceanography Centre, UK, the Swiss Federal Institute of Technology, Oregon State University, University of Alberta, and University of Colorado, Boulder. The project is a component of the NSF Arctic Observing and Atlantic Meridional Overturning Networks, and the international Arctic-Subarctic Ocean Flux (ASOF) program, Global Ocean Ship-Based Hydrographic Investigations Program (GO-SHIP), Global Ocean Acidification Observing Network (GOA-ON), Synoptic Arctic Survey (SAS), Arctic Monitoring Assessment Programme (AMAP), and OceanSITES system.

The observing system employs an array of 12 moorings across Davis Strait, deployed at the locations occupied by the previous arrays (**Figs. 2** and **3**). The mooring array provides estimates of mass, heat, freshwater and ice transports, and marine mammal presence. Bottom pressure recorders deployed along the western and eastern flanks of Davis Strait and in northern Baffin Bay augment the mooring array by providing estimates of barotropic transport through the Strait, constraining interpretation of remotely sensed altimetry and gravity measurements and allowing an investigation of how sea surface height differences between the Arctic and Baffin Bay modulate exchange through Davis Strait. An extensive program of biennial chemical sampling in Davis Strait, northern Labrador Sea, and southern Baffin Bay (**Fig. 2**) quantifies changes in nutrient loads, carbon transport, and acidification, while also providing data for distinguishing freshwater constituents in the Davis outflow. These biogeochemical signals integrate changes in the large-scale circulation (e.g., the ratio of Pacific to Atlantic waters, carbon transport and pH changes). The new system includes a significantly expanded suite of biological and biogeochemical measurements, including dissolved organic matter (DOM), particulate organic carbon (POC), chlorophyll, zooplankton biomass and community structure, phytoplankton productivity, fish larvae and census (from the Canadian Ocean Tracking Network), seabird observations, and marine mammal presence.

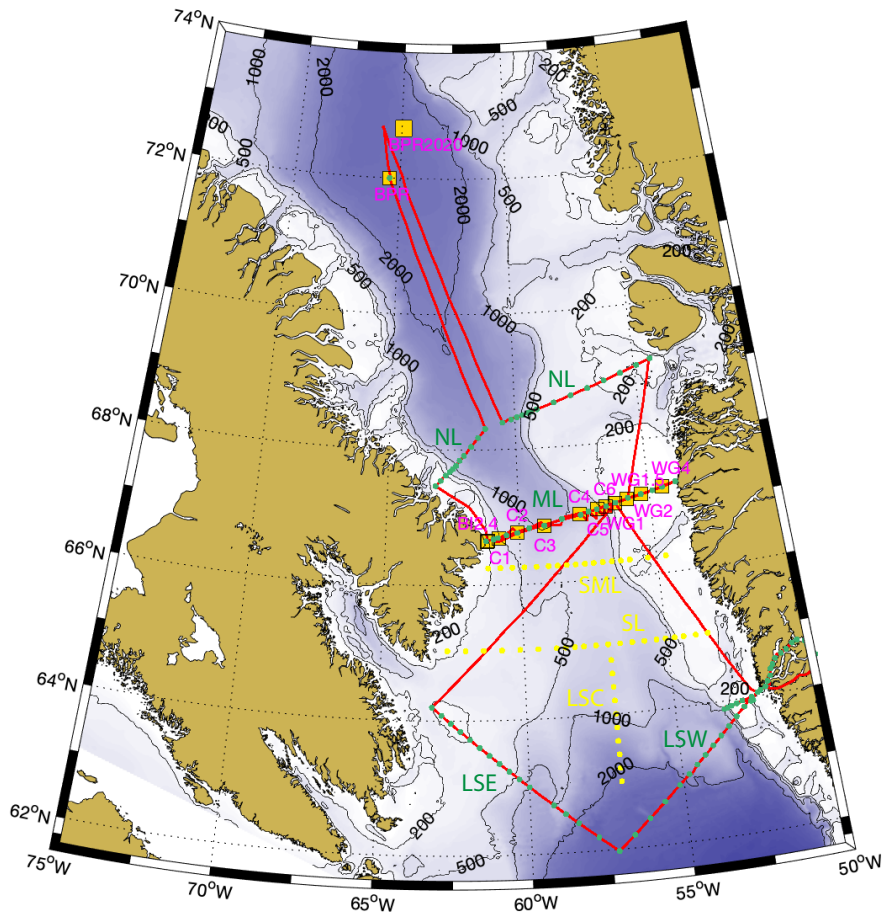


Figure 2. Davis Strait mooring sites (orange squares), and standard hydrographic sampling sections: Northern Line (NL), Mooring Line (ML), Labrador Sea West (LSW), Labrador Sea Central (LSC) and Labrador Sea East (LSE). Yellow and green dots mark CTD stations, with green dots indicating those sampled during the 2022 field program. Two previously sampled sections, the South Mooring Line (SML) and Southern Line (SL), are no longer regularly occupied.

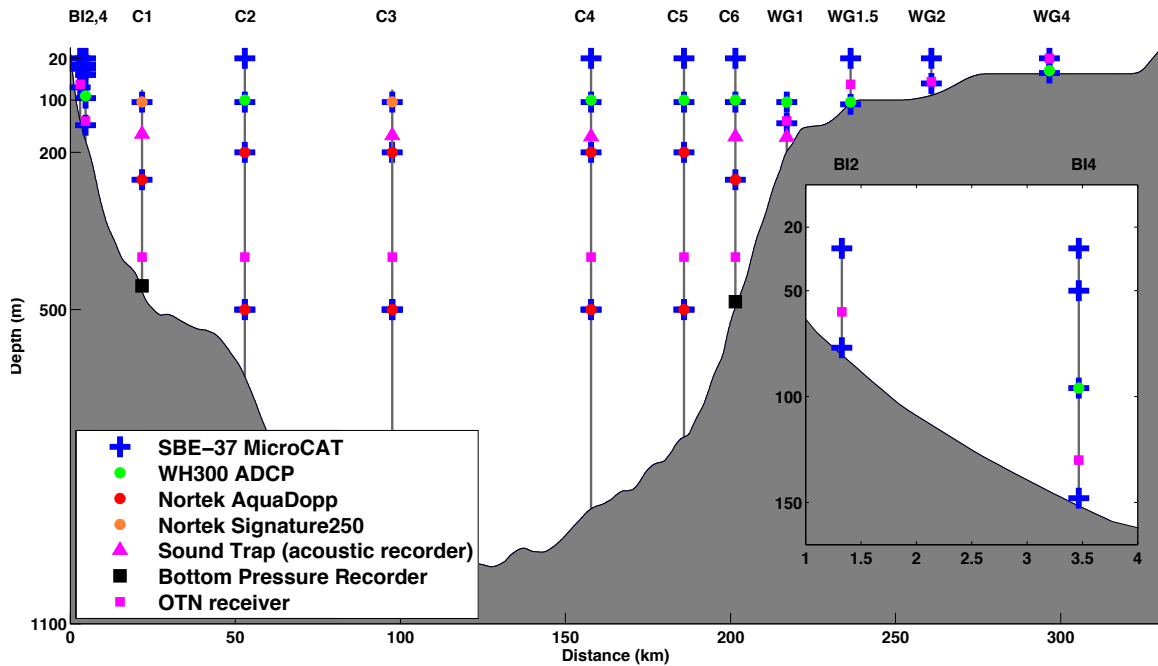


Figure 3. The Davis Strait mooring array. Nortek Signature 250-kHz, 5-beam Doppler current profilers (water velocity profile, ice velocity, and ice draft) replace the WH300 ADCPs and IPS ice sonars previously deployed at C2 and C3. NORTEK AquaDopps replace the RCM11 current meters previously used for deeper current measurements.

In September and October 2022, we undertook the first full-scale scientific expedition under the new phase of the observing system supported by this grant. Previous expeditions under this grant have been limited in scope and personnel due to the global covid-19 pandemic. This expedition included researchers from ten organizations representing seven different countries and, of note, involved eight graduate students and/or early career researchers. For many of these, it was their first formal at-sea oceanographic expedition. The day-to-day cruise narrative is provided in **Appendix 1**.

3. MOORING OPERATIONS

The Davis Strait mooring array consists of thirteen sites (**Fig. 2, Table 1**). A twelve-element array (**Figs. 3 and 4a–m**) spans the Strait, situated north of the sill to avoid recirculation associated with local bathymetry (**Fig. 1**). Moorings are instrumented with Acoustic Doppler Current Profilers (300-kHz Teledyne RDI Workhorse and 250-kHz Nortek Signature) and single point Nortek acoustic current meters to measure

currents, sea ice draft, and velocity. Seabird Electronics SBE37 sensors measure conductivity (salinity), temperature and depth (CTD) at specific points in the water column. Specialized IceCAT systems, designed and fabricated by the IOP group at the Applied Physics Laboratory, University of Washington, collect measurements in the hazardous region near the ice–ocean interface. Each IceCAT consists of a data logger, situated at a depth safe from the sea ice, connected to one or more SBE37 CTDs, at depths near the ice–ocean interface, through an inductive modem and a mechanical weak link. The weak link protects the mooring in the event that the shallow sensors are caught by sea ice, while the inductive link and data logger ensure data recovery regardless of sensor loss. Two moorings, one on each side of the strait (C1, **Fig. 4c** and C6, **Fig. 4h**), carry bottom pressure recorders (BPR) to quantify sea surface height. To investigate the processes that modulate exchange through Davis Strait, an additional BPR mooring (Baffin BPR, **Fig. 4m**) is sited further to the north, in central Baffin Bay (**Fig. 2**).

The entire twelve-element cross-strait array was recovered (**Table 2**) and redeployed (**Table 3**). Due to an error in communicating positions, the 2020 central Baffin Bay BPR site was not recovered in 2022. The 2020 Central Baffin Bay BPR had been deployed in shallower waters northeast of the target site due to issues with MSR permissions. A new Central Baffin Bay BPR mooring was deployed at the original target site (**Table 3**), with recovery of the 2020 instrument deferred until 2023.

Through the UK Natural Environment Research Council BIOPOLE (Biogeochemical processes and ecosystem functioning in changing polar systems and their global impacts, <https://biopole.ac.uk>) project, the National Oceanography Centre (NOC) Southampton expanded the Davis Strait mooring-based measurements to include autonomous water sampling for inorganic (N, P, Si) and organic (N, P) nutrients. Two McLane Research Laboratories Inc. (www.mclane.com) Remote Access Samplers (RAS) 3-48-500, sited at two moorings on the Baffin slope, collect seawater samples at two-week intervals.

Table 1. Davis Strait planned mooring sites 2022.

	Lat (N)	Lon (W)	Bottom (m)	Notes
BI2	66° 38.8'	61° 13.4'	79	
BI4	66° 39.5'	61° 10.2'	152	
WG1	67° 06.4'	56° 19.7'	144	
WG1.5	67° 08.7'	55° 52.7'	111	
WG2	67° 11.6'	55° 18.6'	73	
WG4	67° 15.8'	54° 28.5'	65	
C1	66° 38.5'	60° 46.5'	441	
C2	66° 45.8'	60° 04.7'	656	
C3	66° 51.2'	59° 03.3'	1032	
C4	66° 58.8'	57° 41.5'	866	
C5	67° 02.3'	57° 02.2'	685	
C6	67° 04.2'	56° 40.9'	385	
BPR	72° 00.0'	65° 30.0'	2000+	Alternate sites are: 70° N, 63° W and 69° N, 62° W.

Table 2. Moorings recoveries.

Mooring	Date Deployed (UTC, 2021)	Lat (N)	Lon (W)	Depth	Date Recovered (UTC, 2022)
BI2	4 Aug	66° 38.8'	61° 13.4'	79 m	20:04, 3 Oct
BI4	4 Aug	66° 39.5'	61° 10.2'	152 m	19:40, 3 Oct
C1	10 Sep	66° 38.478'	60° 46.635'	440 m	18:00, 3 Oct
C2	10 Sep	66° 45.548'	60° 04.230'	662 m	15:12, 3 Oct
C3	9 Sep	66° 51.091'	59° 03.305'	1039 m	11:24, 3 Oct
C4	31 Aug	66° 58.511'	57° 40.740'	892 m	20:52, 4 Oct
C5	31 Aug	67° 02.334'	57° 02.558'	704 m	10:38, 6 Oct
C6	30 Aug	67° 04.180'	56° 40.965'	396 m	12:37, 6 Oct
WG1	30 Aug	67° 06.401'	56° 19.640'	150 m	14:18, 6 Oct
WG1.5	30 Aug	67° 08.719'	55° 52.641'	112 m	16:00, 6 Oct
WG2	30 Aug	67° 11.497'	55° 19.082'	75 m	18:02, 6 Oct
WG4	30 Aug	67° 15.703'	54° 29.114'	53 m	20:44, 6 Oct
BPR	4 Sep	72° 44.822'	64° 55.575'	2367 m	Not recovered

Table 3. Mooring deployment dates, surveyed locations, and depth at anchor drop location.

Mooring	Surveyed or Anchor Drop		Deployment Time (UTC, 2022)		Depth (m)	Notes
	Lat (N)	Lon (W)	Start	End		
BI2	66° 38.789'	61° 13.395'	14:47, 12 Oct	14:58, 12 Oct	77	
BI4	66° 39.501'	61° 10.233'	16:20, 12 Oct	16:34, 12 Oct	146	
C1	66° 41.471'	60° 45.964'	19:44, 12 Oct	21:14, 12 Oct	441	Surveyed
C2	66° 45.884'	60° 04.437'	11:15, 13 Oct	12:03, 13 Oct	655	Surveyed
C3	66° 51.113'	59° 03.126'	16:44, 13 Oct	17:40, 13 Oct	1038	Surveyed
C4	66° 58.819'	57° 41.473'	00:00, 14 Oct	01:13, 14 Oct	873	Surveyed
C5	67° 02.284'	57° 02.166'	07:55, 14 Oct	08:46, 14 Oct	688	Surveyed
C6	67° 04.197'	56° 40.867'	11:00, 14 Oct	11:40, 14 Oct	391	Surveyed
WG1	67° 06.400'	56° 19.701'	13:38, 14 Oct	14:02, 14 Oct	147	
WG1.5	67° 08.700'	55° 52.694'	15:22, 14 Oct	15:28, 14 Oct	111	
WG2	67° 11.600'	55° 18.599'	17:05, 14 Oct	17:09, 14 Oct	73	
WG4	67° 15.801'	54° 28.499'	19:26, 14 Oct	19:29, 14 Oct	64	
BPR	71° 59.953'	65° 29.892'	07:20, 10 Oct	07:32, 10 Oct	2322	Surveyed

DS2022 nominal BI-2
 xxxxm depth (CTD) (xxxxm multibeam)
 ()
 nominal:

0m

2 2x Viny 12B-3 floats on wire w/SBE37 (8 kg air wet, 40 kg net positive buoyancy) 30m

45m
 1/4" Nilspin wire rope

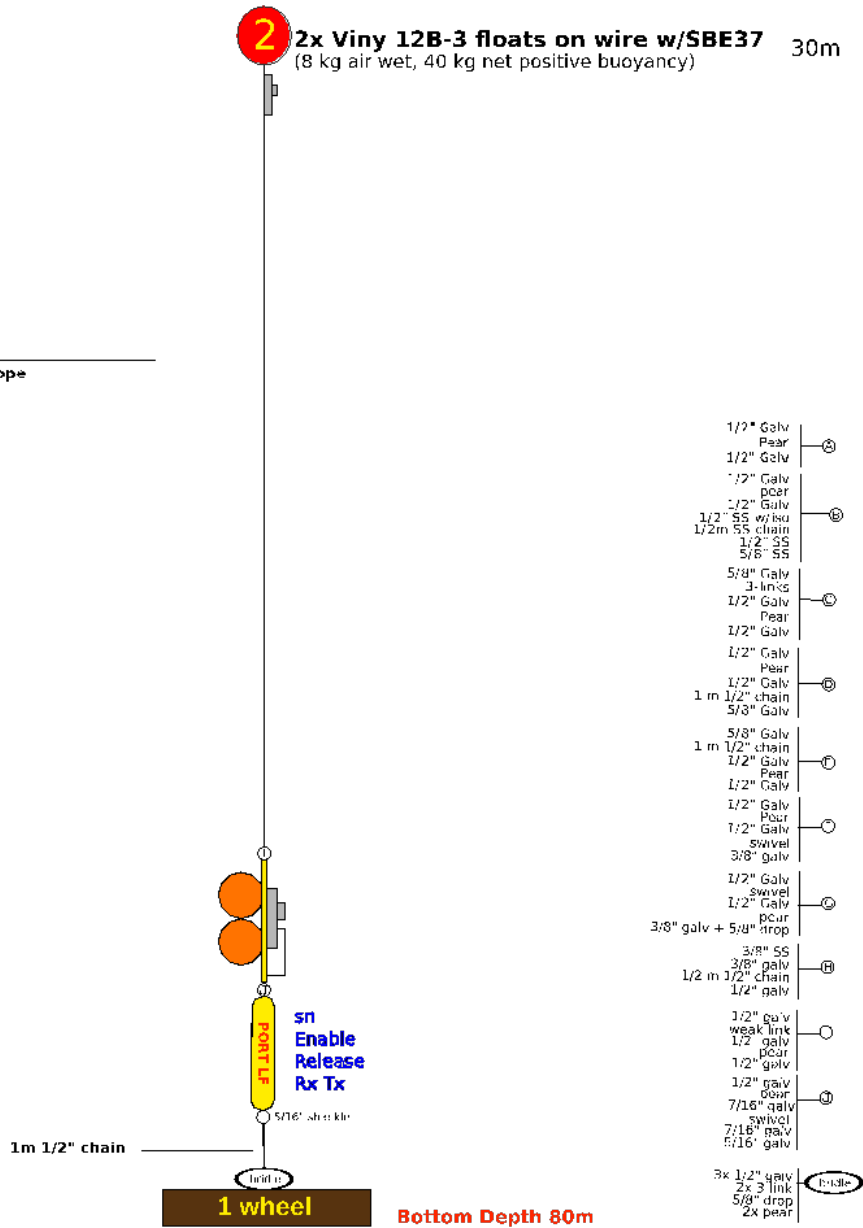


Figure 4a. BI-2 Mooring diagram (Baffin Shelf).

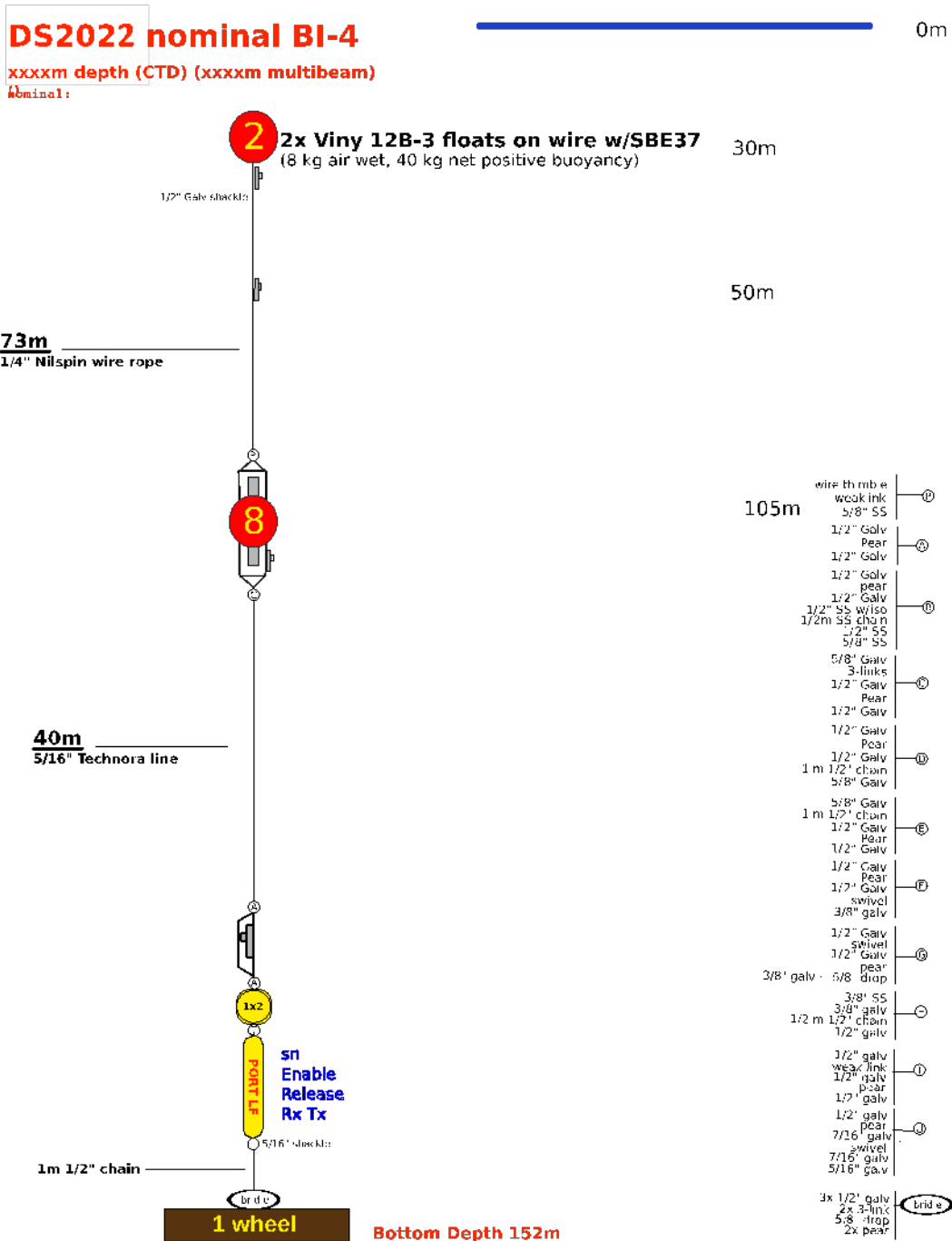


Figure 4b. BI-4 Mooring diagram (Baffin Shelf).

DS2022 nominal C-1
 xxxxm depth (CTD) (xxxxm multibeam)
 0

0m

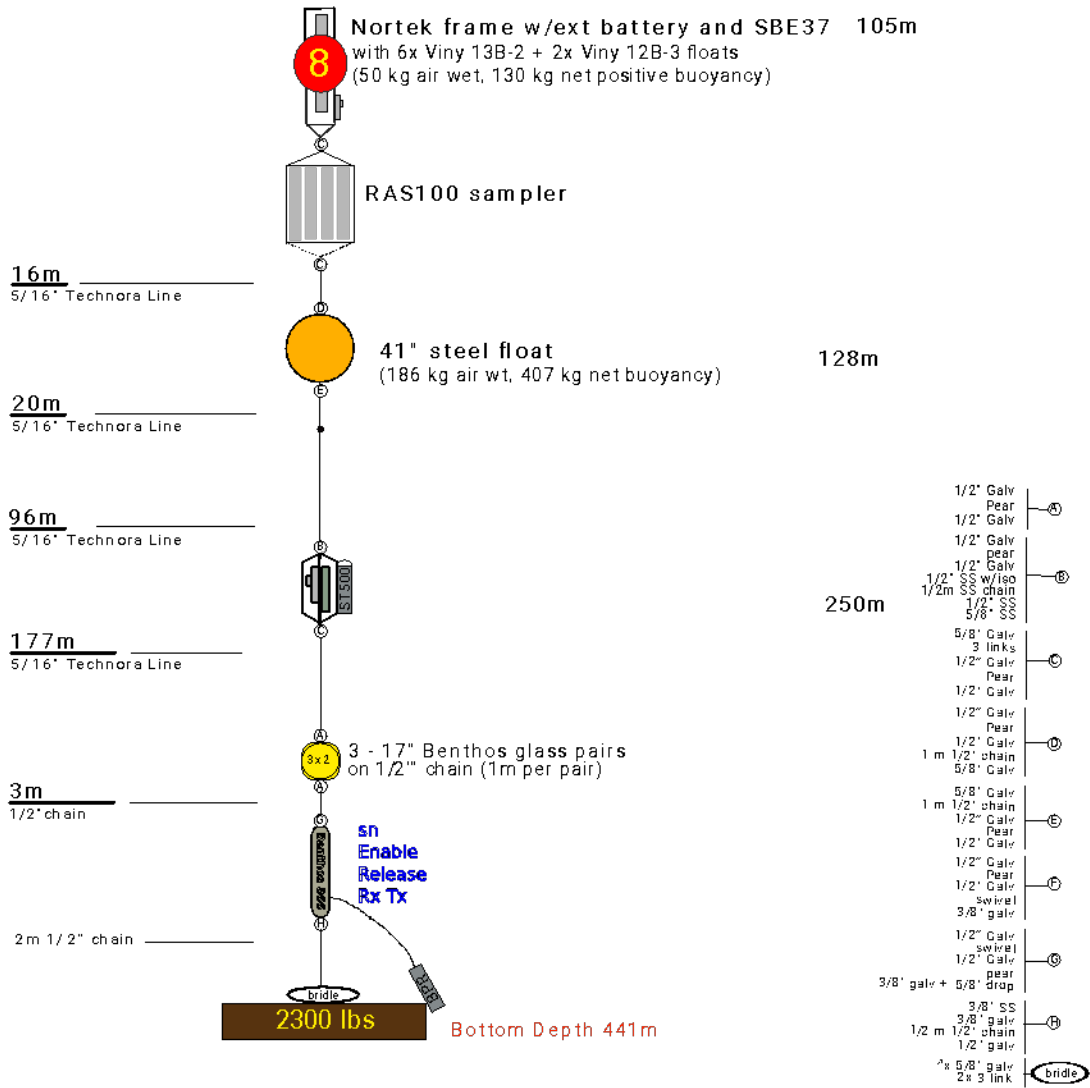


Figure 4c. C1 Mooring diagram.

DS2022 nominal C-2

xxxxm depth (CTD) (xxxxm multibeam)
(1)

0m

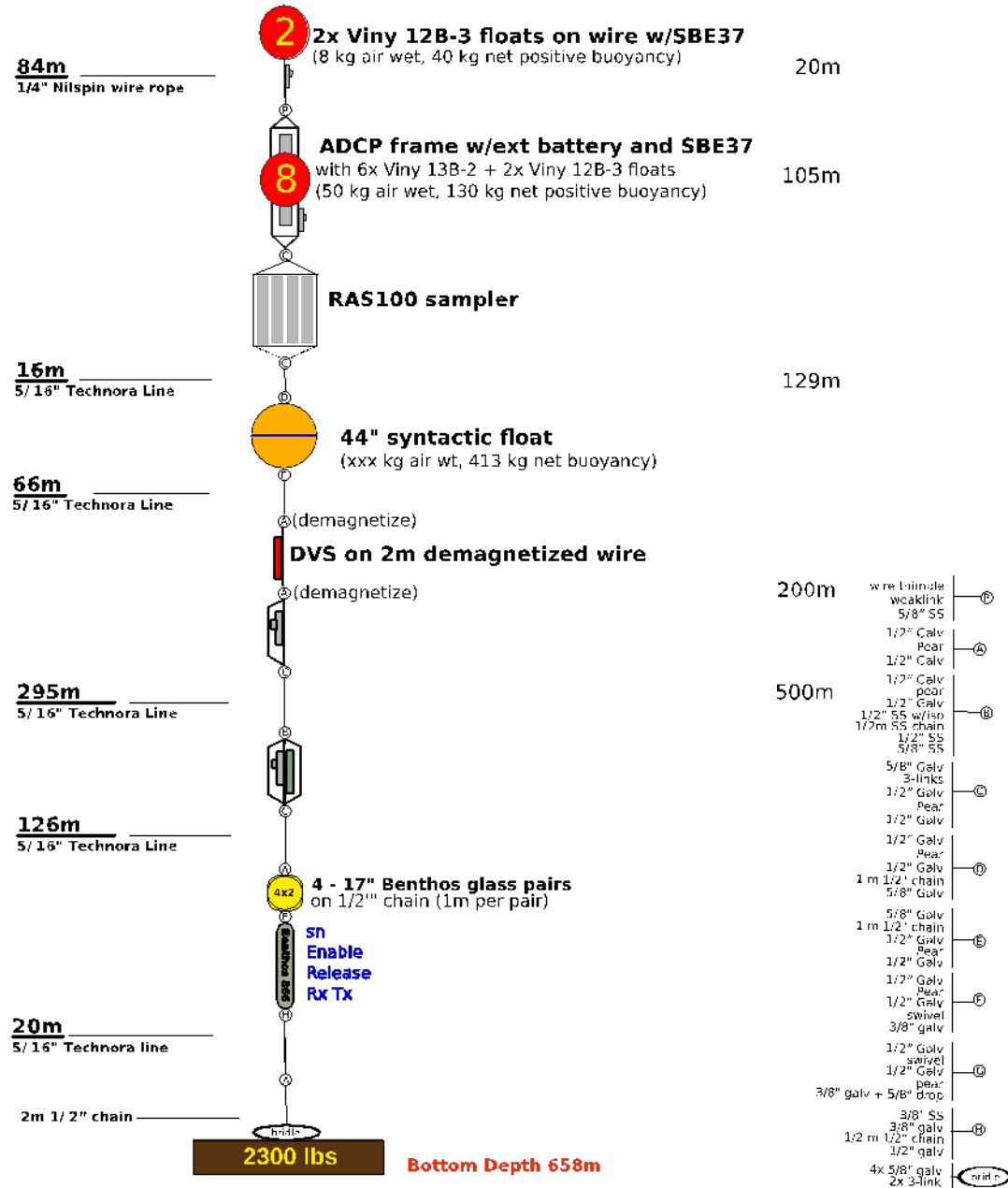


Figure 4d. C2 Mooring diagram.

DS2022 nominal C-4
 xxxxm depth (CTD) (xxxxm multibeam)
 (1)

0m

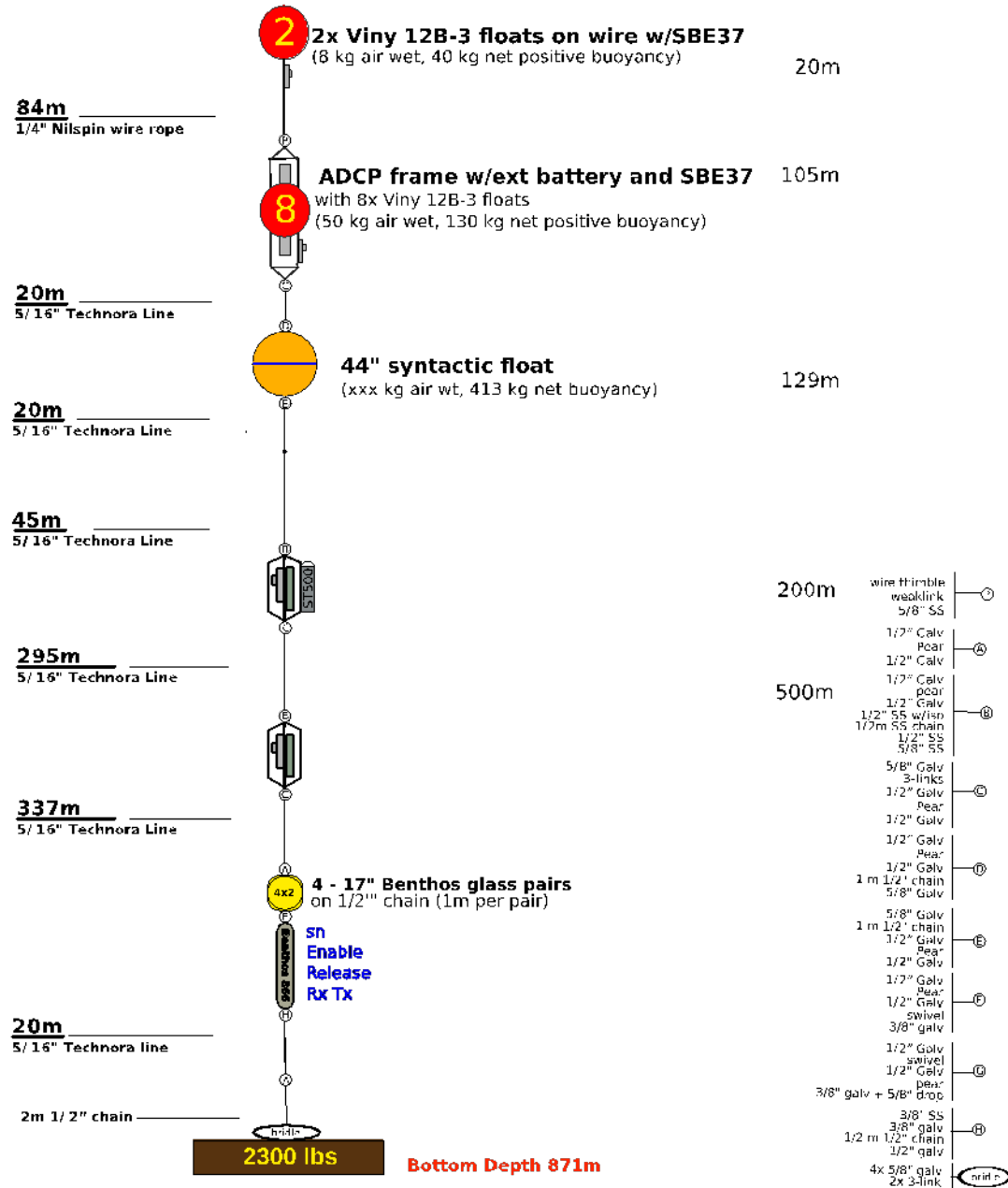


Figure 4f. C4 Mooring diagram.

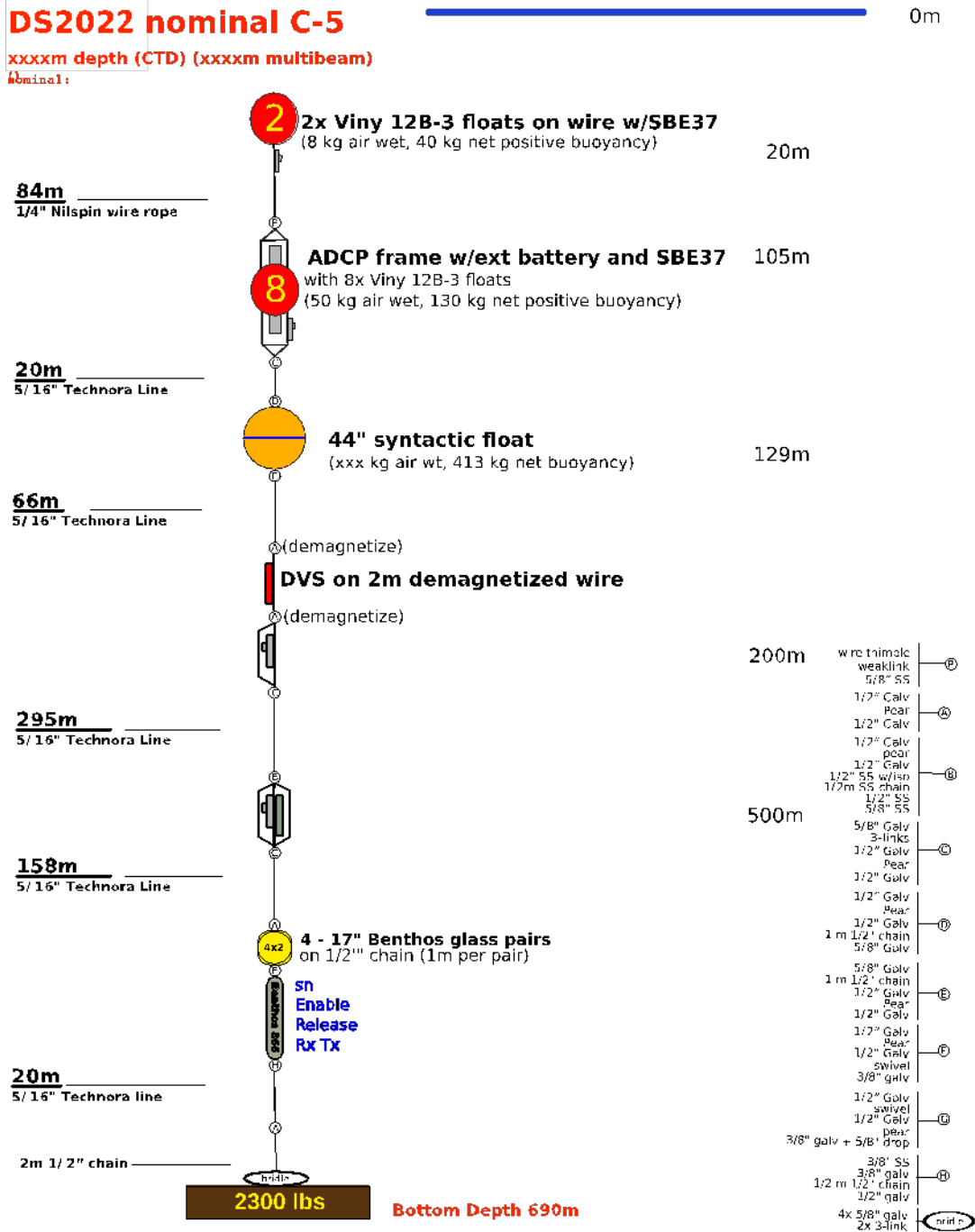


Figure 4g. C5 Mooring diagram.

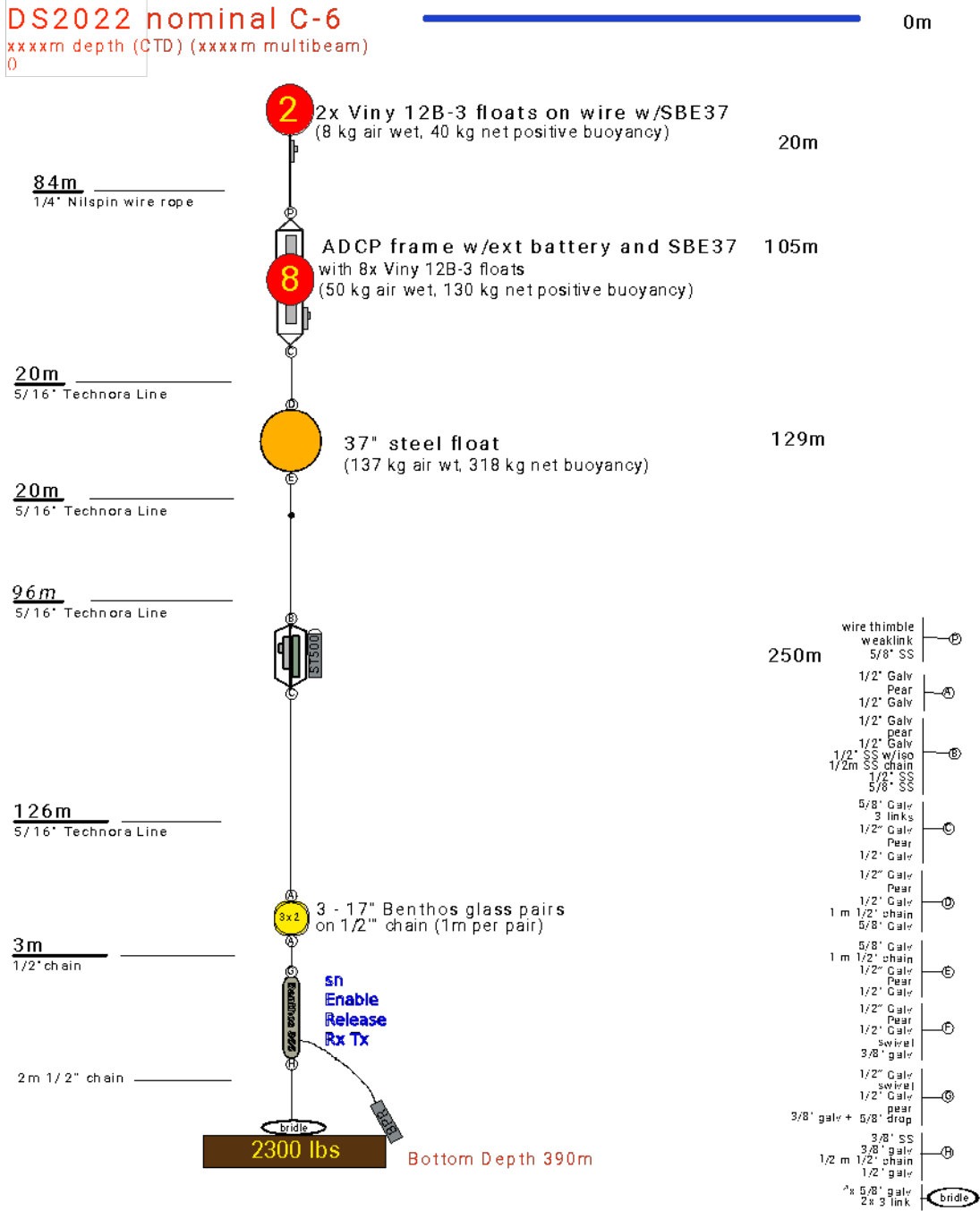


Figure 4h. C6 Mooring diagram.

DS2022 nominal WG-1

xxxxm depth (CTD) (xxxxm multibeam)
 nominal:

0m

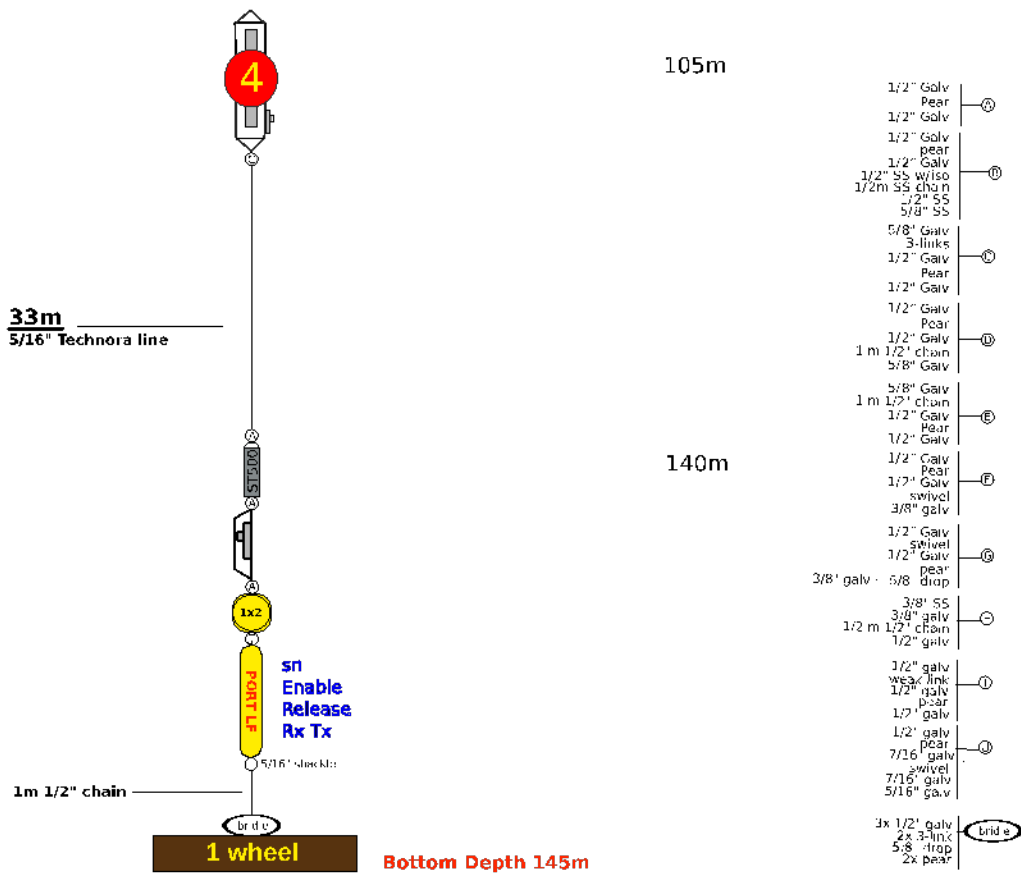


Figure 4i. WG-1 Mooring diagram (West Greenland Shelf).

DS2022 nominal WG-1.5

xxxxm depth (CTD) (xxxxm multibeam)
 terminal:

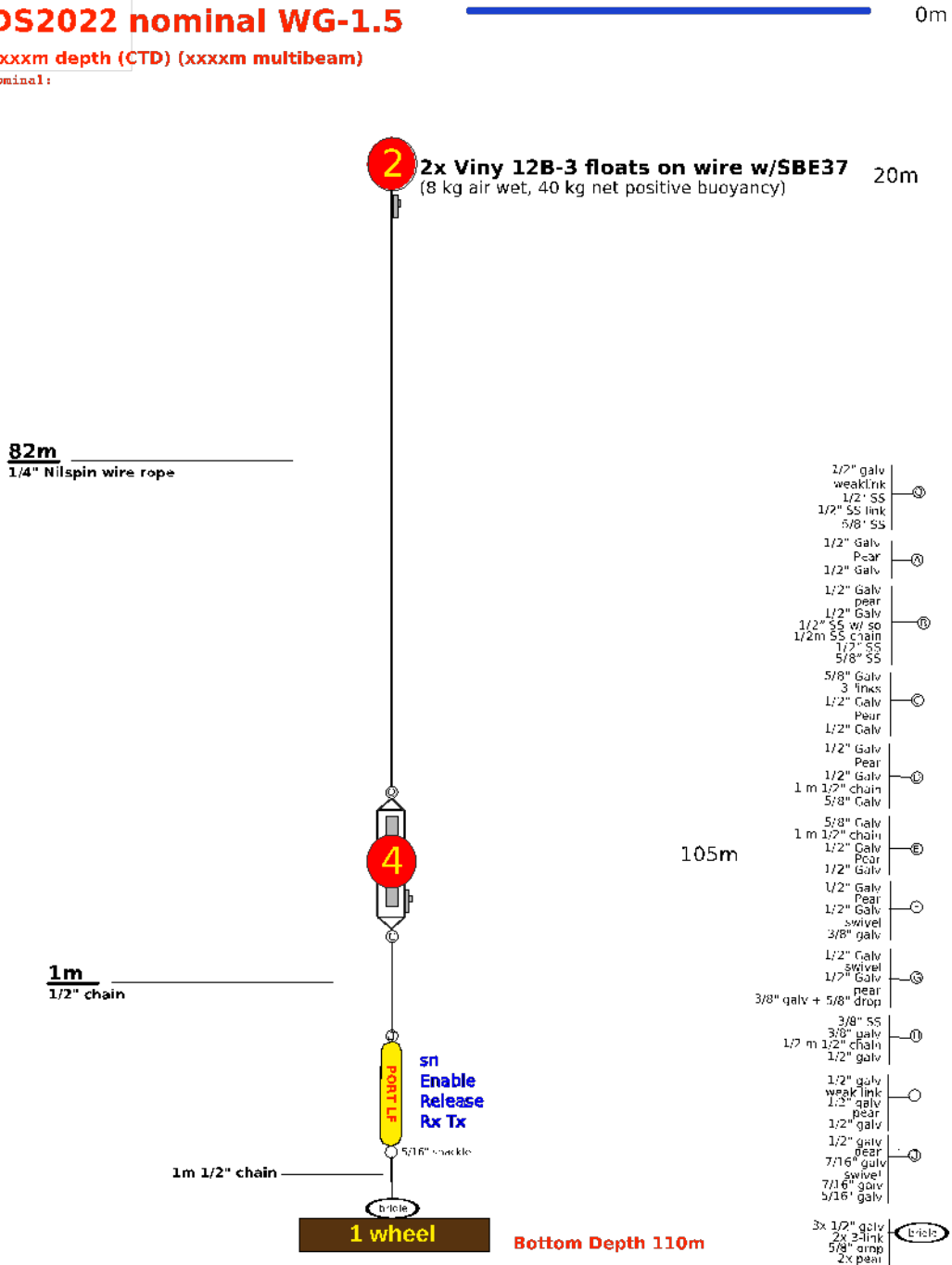


Figure 4j. WG-1.5 Mooring diagram (West Greenland Shelf).

DS2022 nominal WG-2

xxxxm depth (CTD) (xxxxm multibeam)
()
nominal:

0m

49m
1/4" Nilspin wire rope

2 2x Viny 12B-3 floats on wire w/SBE37 (8 kg air wet, 40 kg net positive buoyancy) 20m

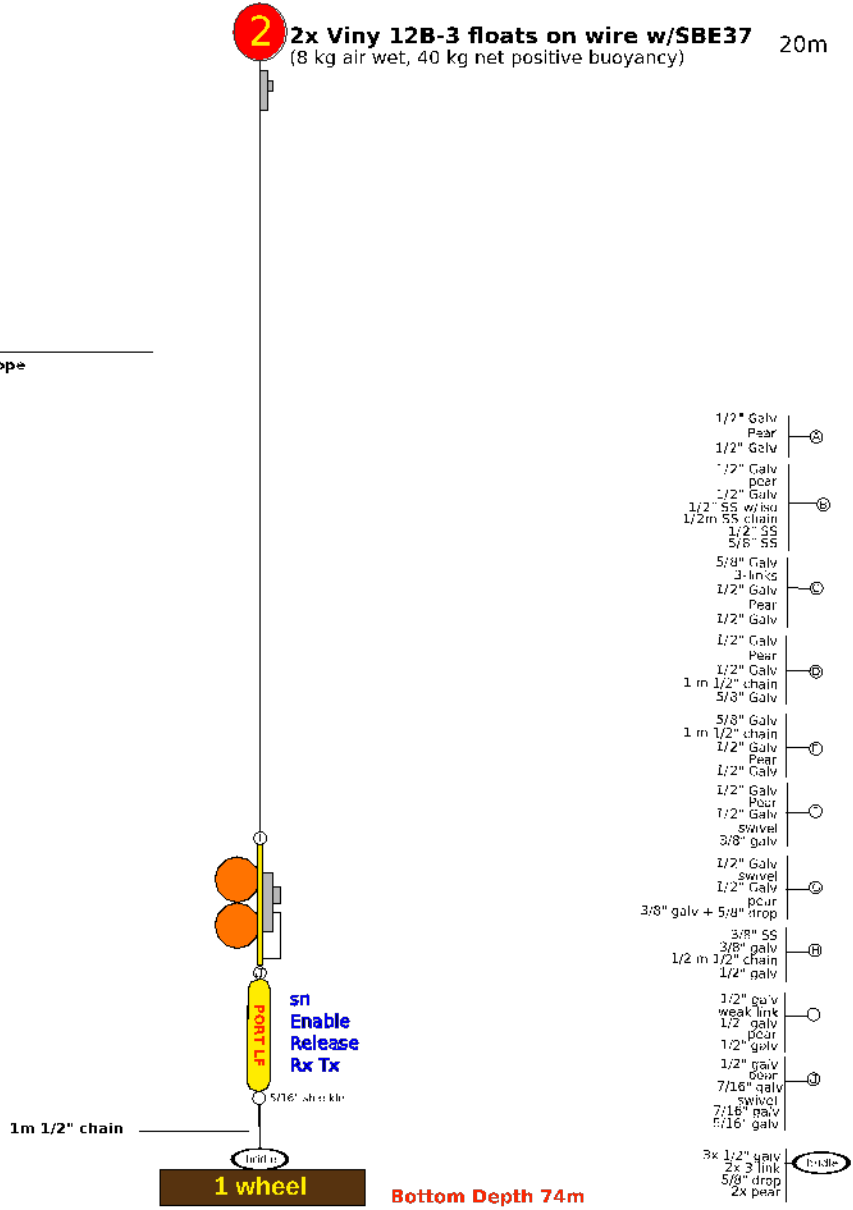


Figure 4k. WG-2 Mooring diagram (West Greenland Shelf).

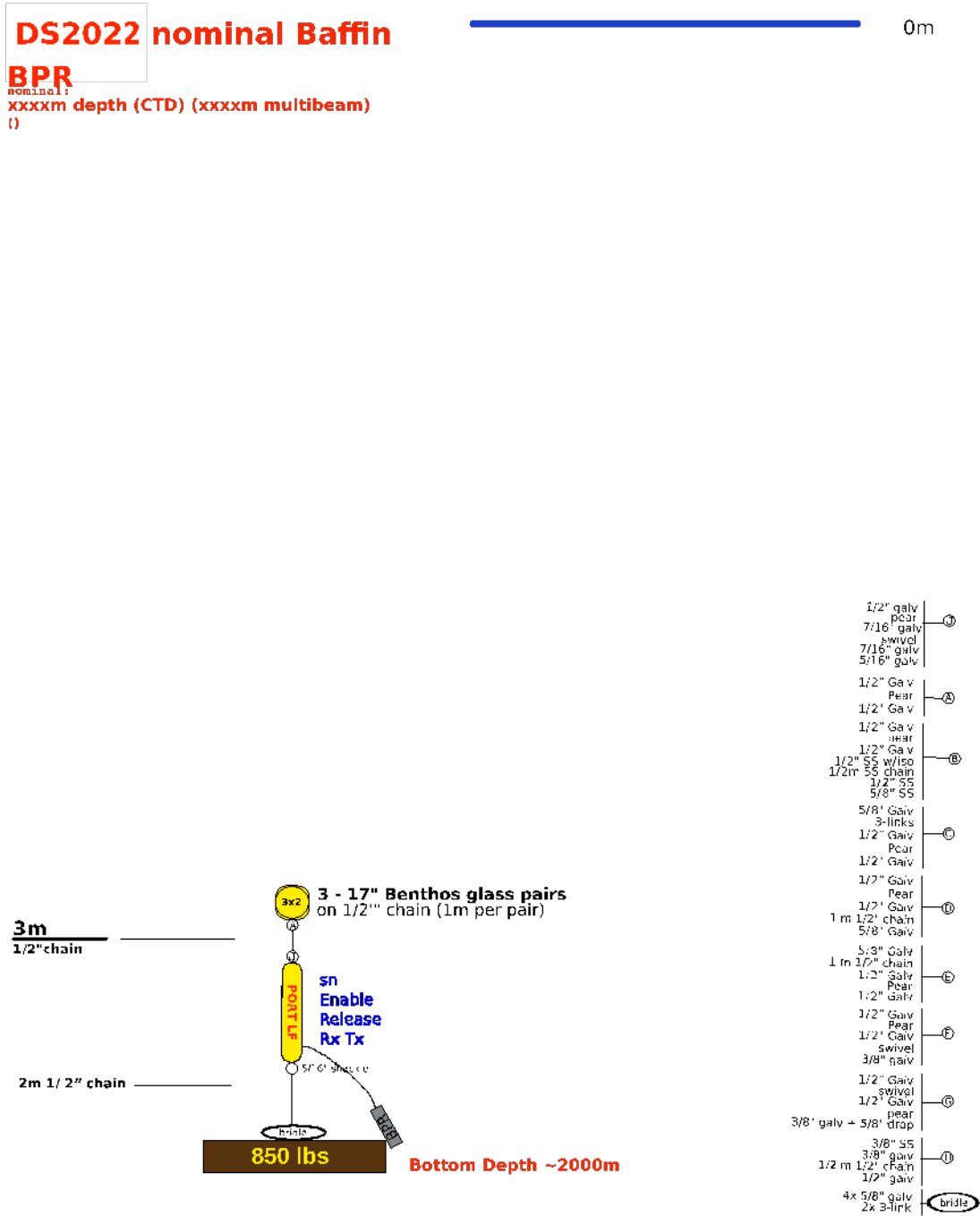


Figure 4m. BPR Mooring diagram (central Baffin Bay).

4. HYDROGRAPHIC SAMPLING

Biennial hydrographic sampling focuses on the Northern Labrador Sea, Davis Strait Mooring Line, and southern Baffin Bay, continuing the occupation of sections established during the first phase (2004–2015) of the program (Figs. 2, 5, and 6–11). The program has de-prioritized the Southern Mooring (Ross line) and Southern Lines, and severe weather prevented sampling of the northern Labrador Sea Central (LCS) section. While R/V *Armstrong* sheltered within the fjords near Nukk, we sampled sections across Fyllas Bank and inside Gothåbsfjord and Ameralik Fjord (Fig. 5). These repeat stations are occupied routinely by the Greenland Institute of Natural Resources.

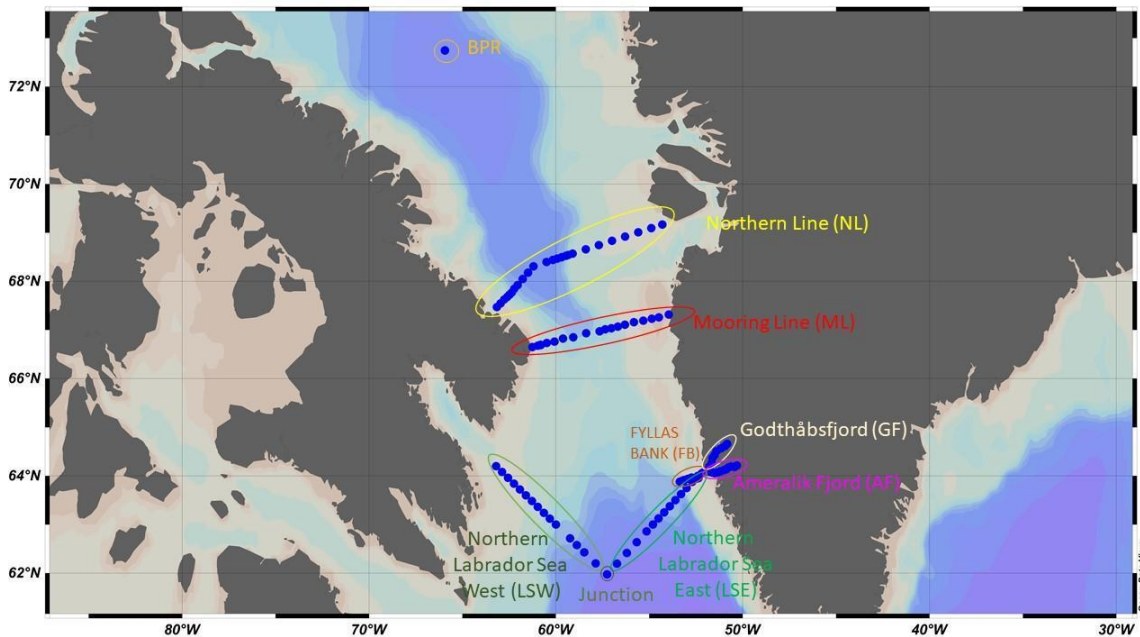


Figure 5. CTD/rosette stations.

Hydrographic sampling employed a Seabird Electronics 911+ CTD system paired with a 24-place, 10 L rosette. Sensors included conductivity/salinity, temperature, pressure, oxygen (SBE 43), fluorescence (WET Labs ECO-AFL/FL), beam transmission/attenuation (WET Labs C-Star), PAR/irradiance (Biospherical/Licor), pH (SBE18) and CDOM (WET Labs CDOM). Chemical parameters collected included total inorganic carbon (TIC), total alkalinity (TA), dissolved organic matter (DOM), dissolved oxygen (DO), ^{18}O , nutrients, underway pCO_2 , radionuclides (^{129}I , ^{236}U and ^{14}C), barium, rare earth elements (REE), neodymium, dissolved organic nitrogen, and dissolved organic phosphate and salinity. A total of 105 CTD/rosette casts were conducted at 102 stations

(Fig. 4) and water samples were collected from 1180 separate Niskin bottles. Cast numbers and station names in 2022 are summarized in **Tables 4–7**.

Malfunction of the oxygen sensor was suspected for the stations from LSW15 (cast 62) to FB01 (cast 82). A ship technician (WHOI SSSG) cleaned the surface/tube and it seemed to perform well after cast 83. Post-cruise calibration with Winkler measurements needs to be performed carefully for casts 62–83, which had suspect O₂ values. Salinity, CDOM, and pH profiles will be calibrated using water samples.

Table 4. Mooring Line (ML) CTD sites.

	Lat (N)	Lon (W)	Bottom (m)	Notes
ML01	66° 39.1'	061° 15.4'	69	Nets
ML02	66° 40.5'	060° 58.4'	376	Nets
ML03	66° 41.7'	060° 48.9'	438	Nets
ML04	66° 43.9'	060° 29.0'	536	
ML05	66° 45.6'	060° 04.3'	662	Nets
ML06	66° 49.5'	059° 37.4'	919	
ML07	66° 51.1'	059° 03.4'	1035	Nets
ML08	66° 56.0'	058° 22.7'	1015	
ML09	66° 58.5'	057° 39.8'	861	
ML10	67° 00.8'	057° 21.5'	801	
ML11	67° 02.1'	057° 02.3'	686	Nets
ML12	67° 04.1'	056° 40.5'	394	Nets
ML13	67° 06.4'	056° 18.8'	156	Nets
ML14	67° 09.6'	055° 49.4'	118	
ML15	67° 11.5'	055° 19.1'	75	
ML16	67° 13.8'	054° 51.9'	56	
ML17	67° 15.7'	054° 29.1'	56	Nets
ML18	67° 19.0'	053° 57.2'	28	

Table 5. Northern Line (NL) CTD sites.

	Lat (N)	Lon (W)	Bottom (m)	Notes
NL01	67° 28.2'	063° 09.4'	56	
NL02	67° 32.8'	062° 57.8'	98	No water sampling
NL03	67° 37.5'	062° 46.1'	135	Nets
NL04	67° 40.63'	062° 36.6'	666	No water sampling
NL05	67° 43.4'	062° 29.2'	911	
NL06	67° 46.1'	062° 21.9'	1006	No water sampling
NL07	67° 50.8'	062° 13.5'	1091	
NL08	67° 55.1'	062° 03.4'	1410	No water sampling
NL09	68° 02.9'	061° 46.2'	1656	
NL10	68° 10.7'	061° 29.1'	1700	
NL11	68° 18.5'	061° 12.0'	1692	Second surface CTD, nets
NL12	68° 23. 7'	060° 29.9'	1599	
NL13	68° 26.3'	060° 09.1'	1449	
NL14	68° 28.0'	059° 55.3'	1265	No water sampling
NL15	68° 29.8'	059° 41.4'	887	
NL16	68° 31.5'	059° 27.5'	592	No water sampling
NL17	68° 32.4'	059° 20.6'	514	Nets
NL18	68° 34.2'	059° 05.8'	299	No water sampling
NL19	68° 39.4'	058° 23.8'	312	
NL20	68° 44.7'	057° 41.7'	295	No water sampling
NL21	68° 49.9'	056° 59.7'	287	
NL22	68° 55.1'	056° 17.6'	168	No water sampling
NL23	69° 00.4'	055° 35.6'	134	Nets
NL24	69° 05.6'	054° 53.5'	177	No water sampling
NL25	69° 10.0'	054° 18.0'	112	

Table 6. Labrador Sea West (LSW) Line CTD sites.

	Lat (N)	Lon (W)	Bottom (m)	Notes
LSW01	64° 12.0'	063° 12.0'	215	
LSW02	64° 04.8'	062° 52.8'	146	
LSW03	63° 57.6'	062° 33.6'	158	Nets
LSW04	63° 50.4'	062° 14.4'	186	No water sampling
LSW05	63° 43.2'	061° 55.2'	200	
LSW06	63° 36.0'	061° 36.0'	215	No water sampling
LSW07	63° 28.8'	061° 16.8'	306	
LSW08	63° 21.6'	060° 57.6'	377	No water sampling
LSW09	63° 14.4'	060° 38.4'	386	
LSW10	63° 07.2'	060° 19.2'	724	Nets
LSW11	63° 00.0'	060° 00.0'	1151	
LSW12	62° 42.9'	059° 14.3'	1013	
LSW13	62° 34.6'	058° 52.6'	1344	
LSW14	62° 25.7'	058° 28.6'	2101	
LSW15	62° 12.1'	057° 52.2'	2449	
JUNC	61° 58.44'	057° 15.8'	2546	Junction between LSW, LSE, and LSC

Table 7. Labrador Sea East (LSE) Line CTD sites.

	Lat (N)	Lon (W)	Bottom (m)	Notes
LSE01	62° 11.7'	056° 44.0'	2482	Nets
LSE02	62° 24.9'	056° 12.2'	2574	No water sampling
LSE03	62° 38.2'	055° 40.4'	2429	
LSE04	62° 51.4'	055° 08.6'	2364	No water sampling
LSE05	63° 00.0'	054° 48.0'	1752	
LSE06	63° 07.5'	054° 30.0'	1427	No water sampling
LSE07	63° 15.0'	054° 12.0'	1171	
LSE08	63° 22.5'	053° 54.0'	1028	No water sampling
LSE09	63° 30.0'	053° 36.0'	1182	
LSE10	63° 37.5'	053° 18.0'	1194	
LSE11	63° 45.0'	053° 00.0'	146	Nets
LSE12	63° 52.5'	052° 42.0'	49	Nets
LSE13	64° 00.0'	052° 24.0'	83	

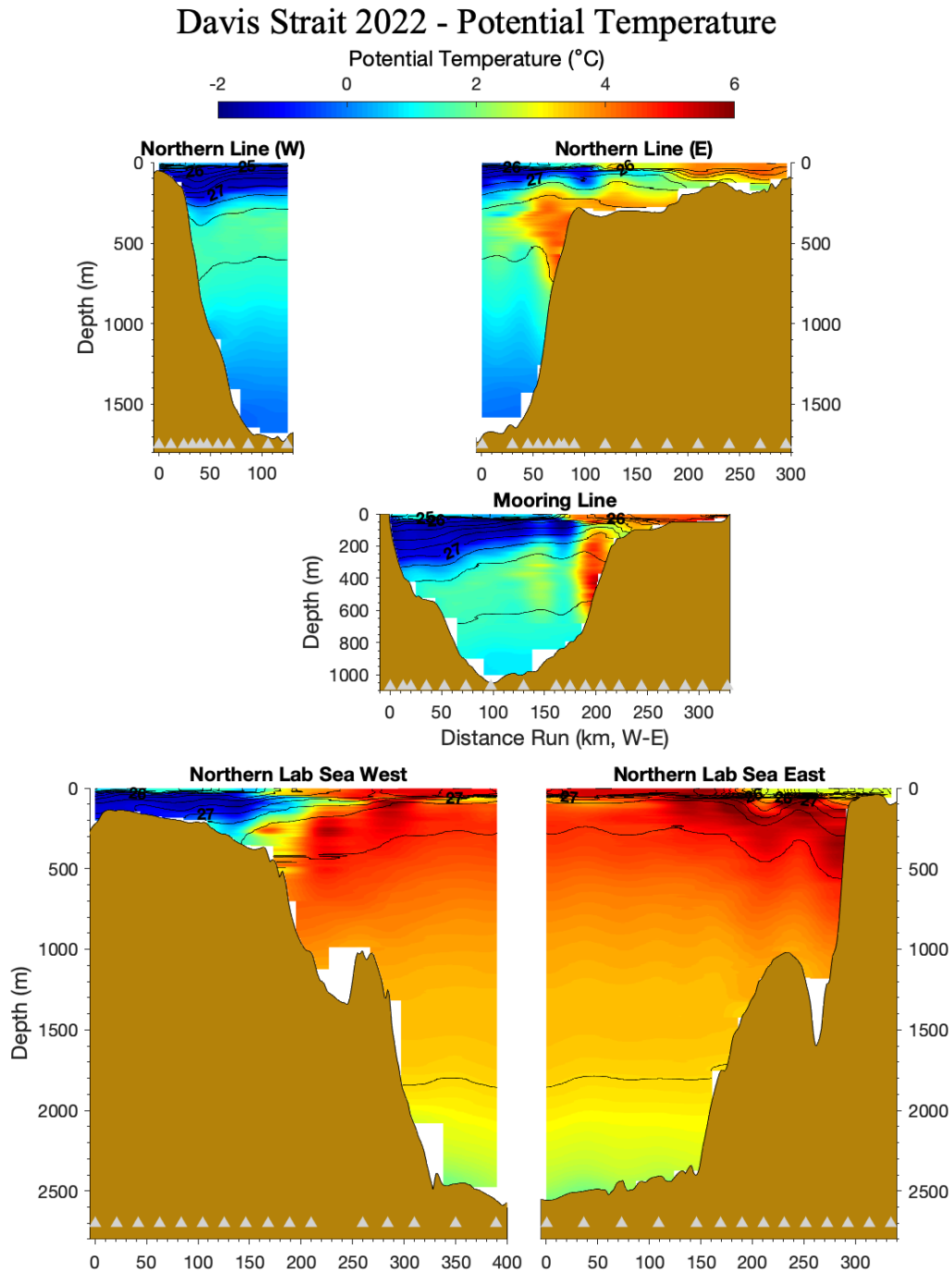


Figure 6a. Potential temperature (°C) along the Northern, Mooring, and West/East Labrador Sea sections. Gray triangles mark station locations.

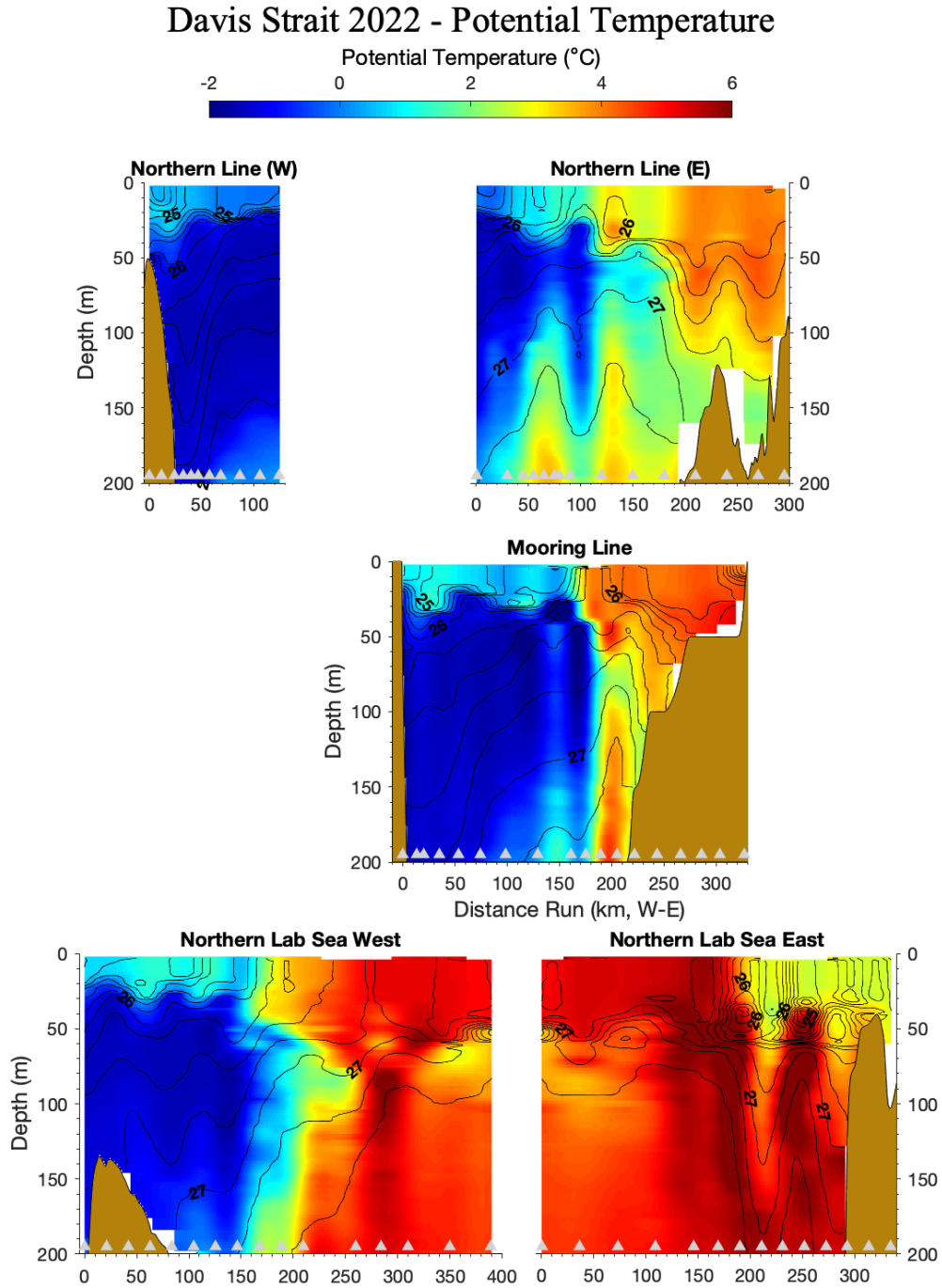


Figure 6b. Potential temperature (°C) of the upper 200 m along the Northern, Mooring, and West/East Labrador Sea sections. Gray triangles mark station locations.

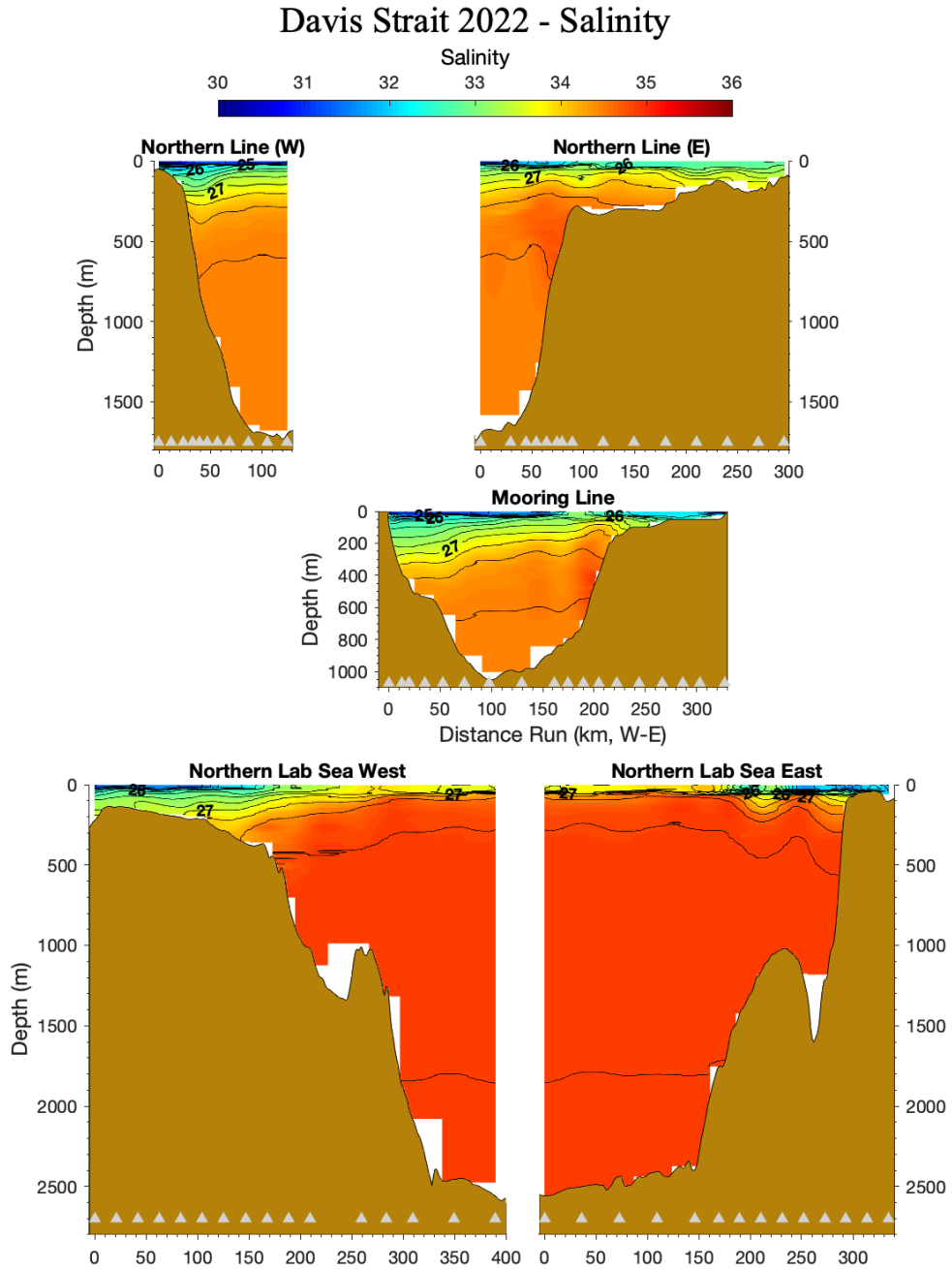


Figure 7a. Salinity (psu) along the Northern, Mooring, and West/East Labrador Sea sections. Gray triangles mark station locations.

Davis Strait 2022 - Salinity

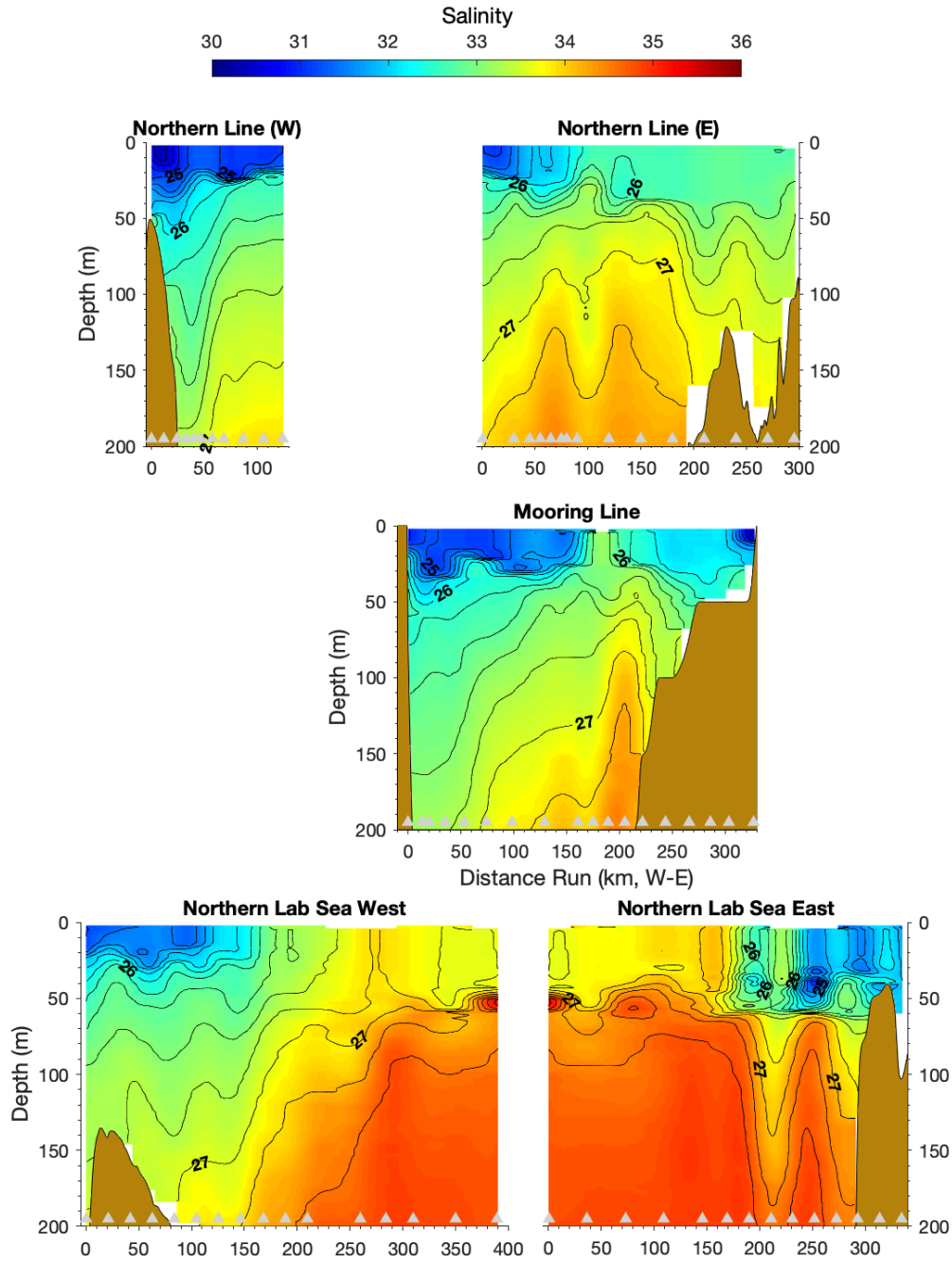


Figure 7b. Salinity (psu) of the upper 200 m along the Northern, Mooring, and West/East Labrador Sea sections. Gray triangles mark station locations.

Davis Strait 2022 - Dissolved Oxygen

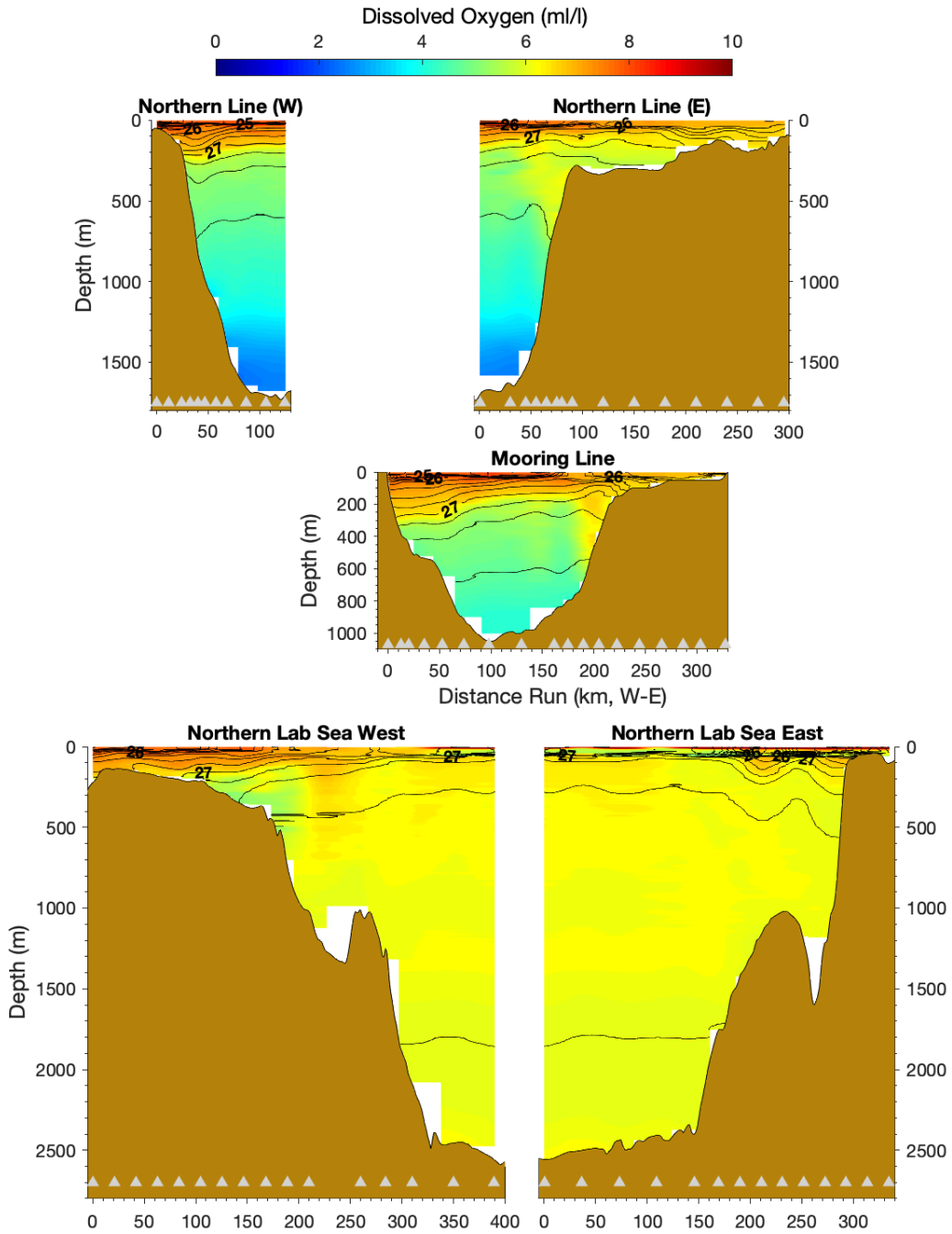


Figure 8a. Dissolved oxygen (ml/L) along the Northern, Mooring, and West/East Labrador Sea sections. Gray triangles mark station locations.

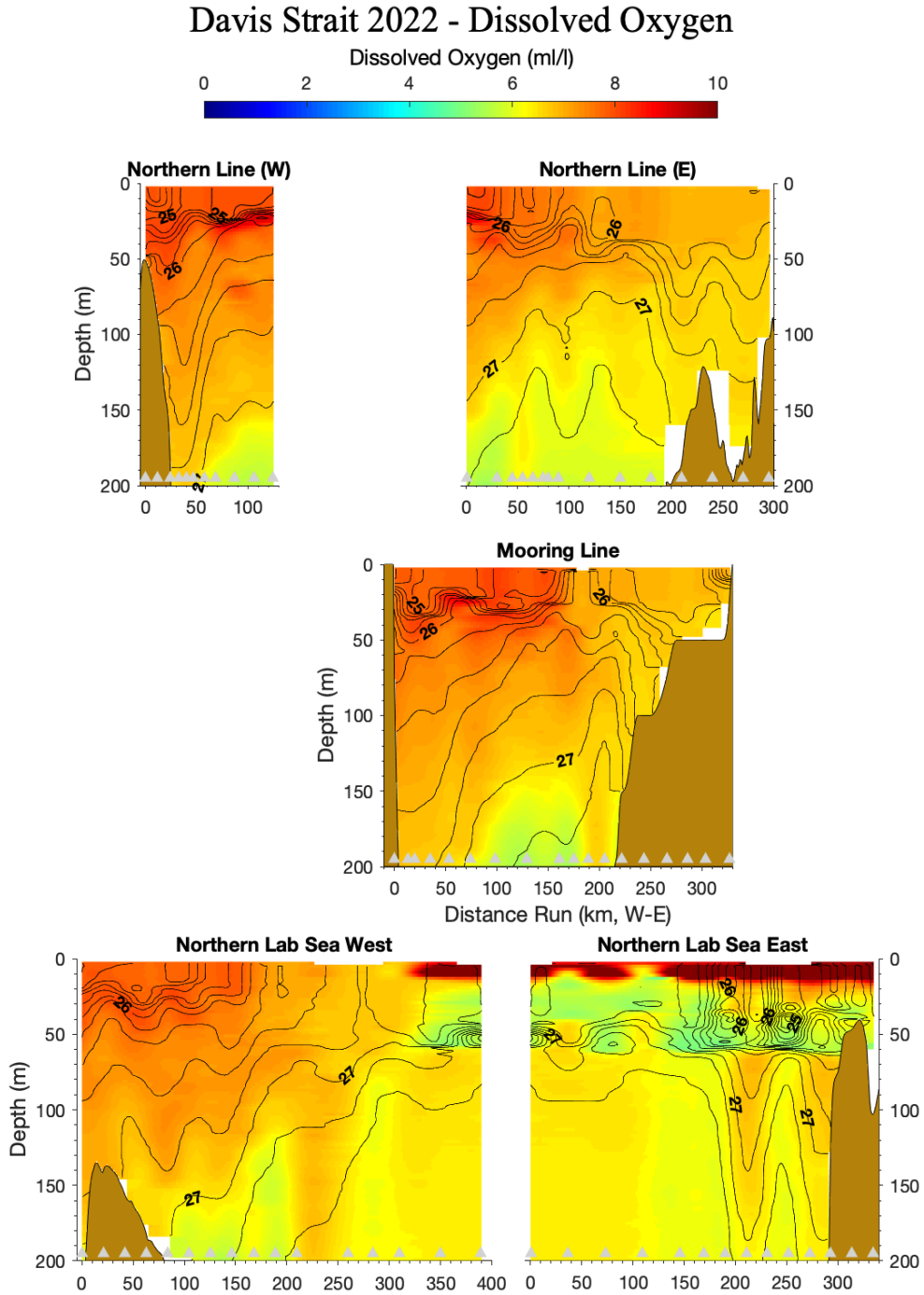


Figure 8b. Dissolved oxygen (ml/L) of the upper 200 m along the Northern, Mooring, and West/East Labrador Sea sections. Gray triangles mark station locations.

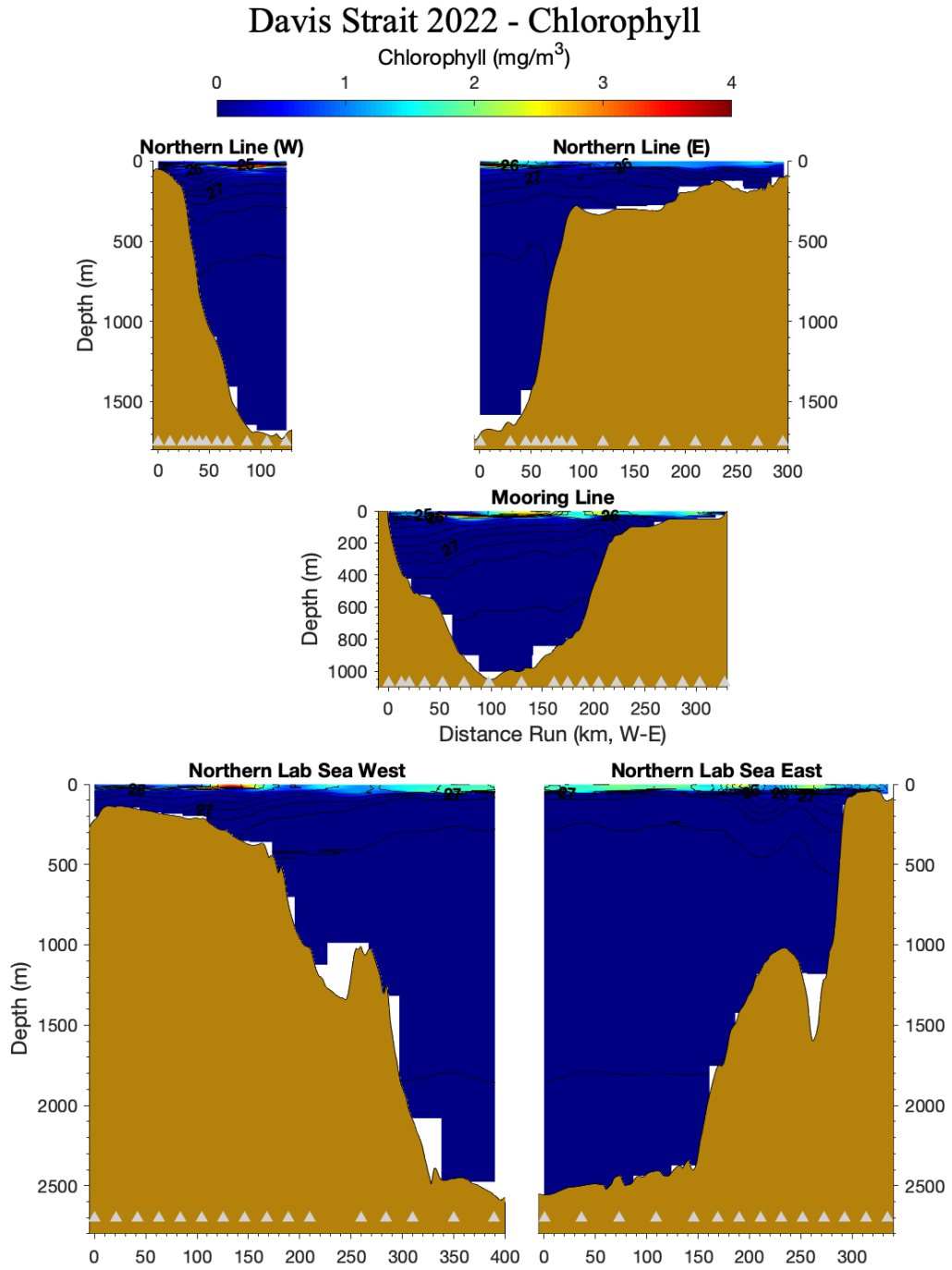


Figure 9a. Chlorophyll fluorescence (mg/m^3) along the Northern, Mooring, and West/East Labrador Sea sections. Gray triangles mark station locations.

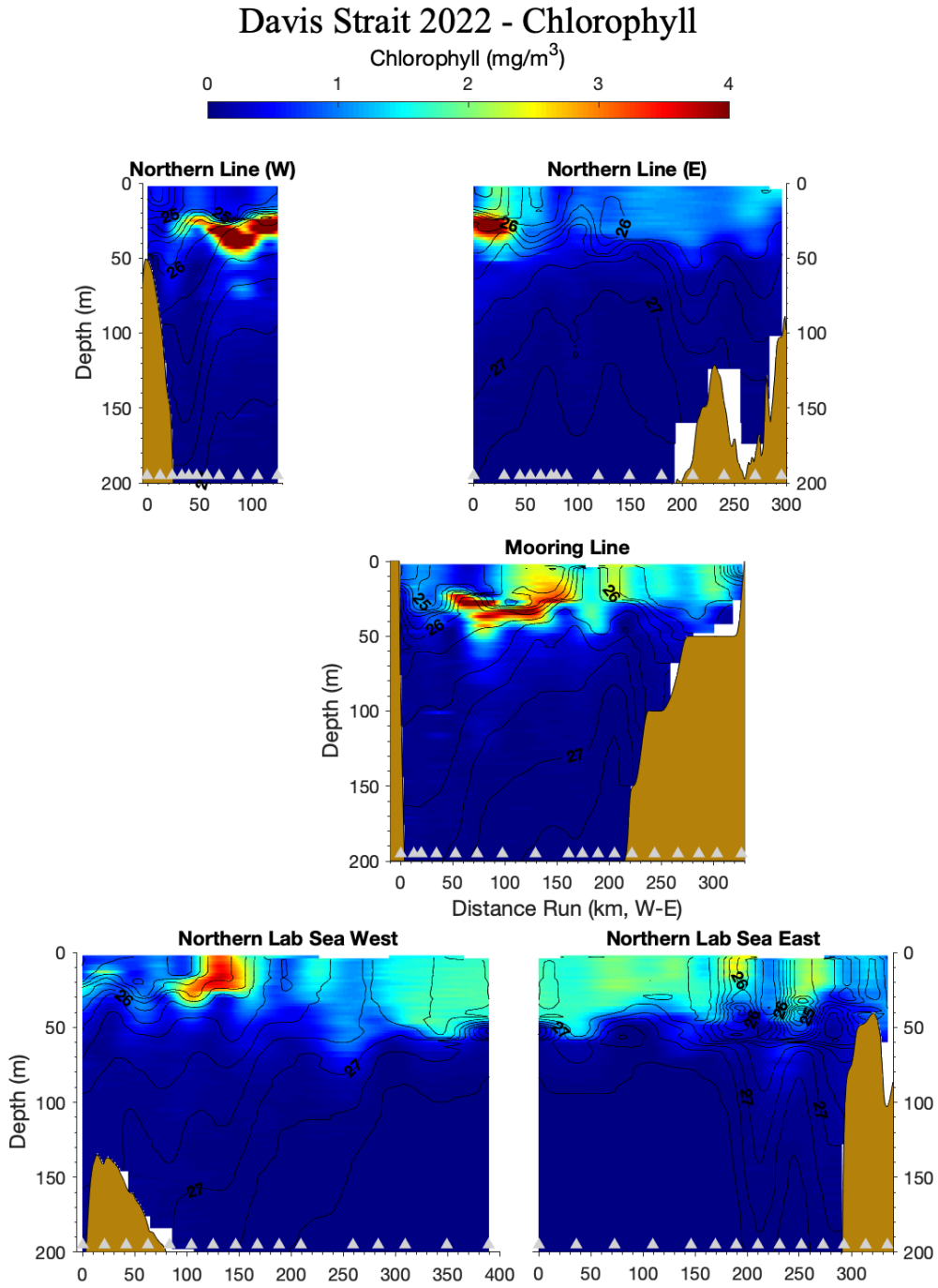


Figure 9b. Chlorophyll fluorescence (mg/m^3) of the upper 200 m along the Northern, Mooring, and West/East Labrador Sea sections. Gray triangles mark station locations.

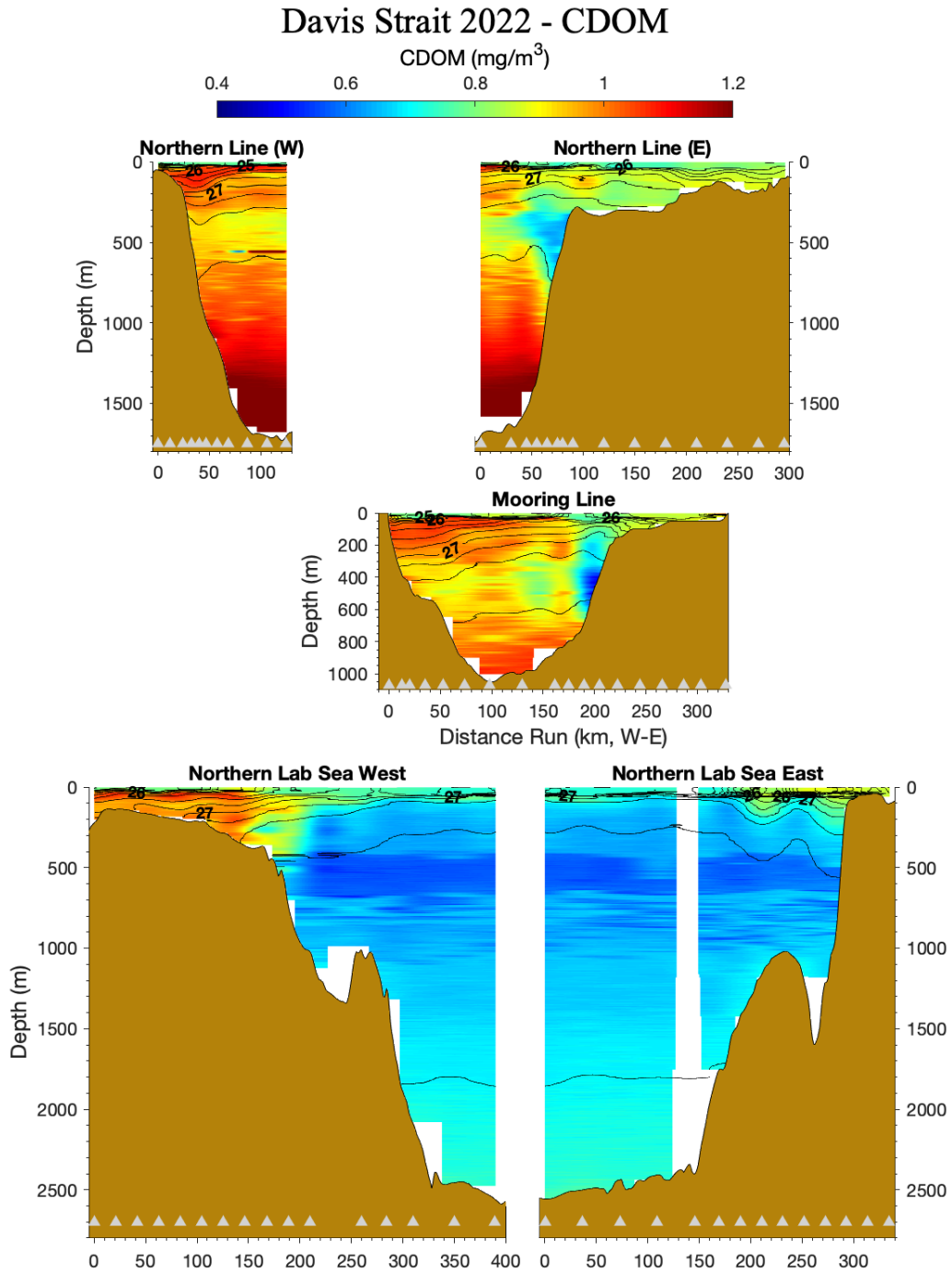


Figure 10a. CDOM fluorescence (mg/m^3) along the Northern, Mooring, and West/East Labrador Sea sections. Gray triangles mark station locations.

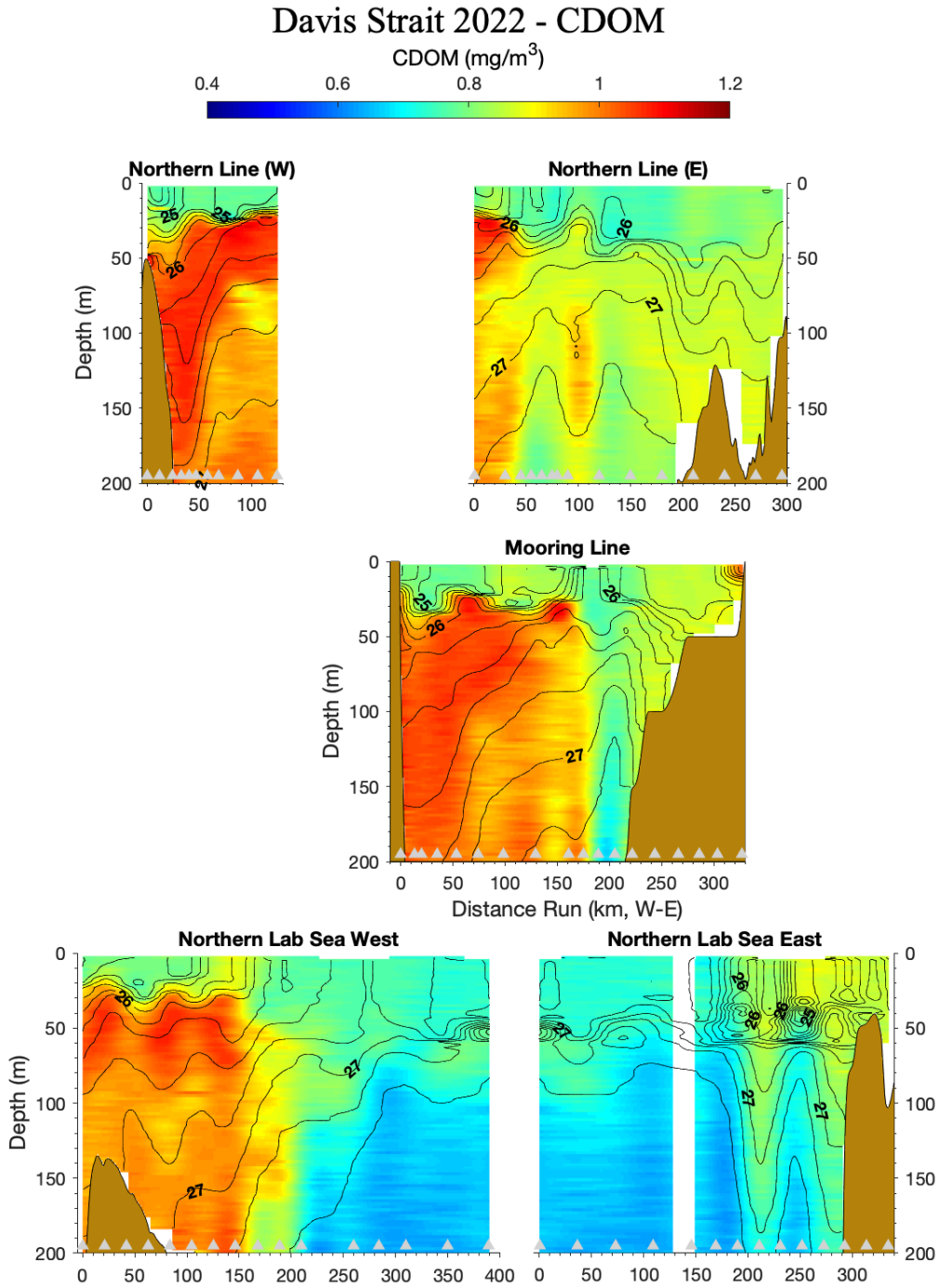


Figure 10b. CDOM fluorescence (mg/m³) of the upper 200 m along the Northern, Mooring, and West/East Labrador Sea sections. Gray triangles mark station locations.

Davis Strait 2022 - Light Transmission (beam-c)

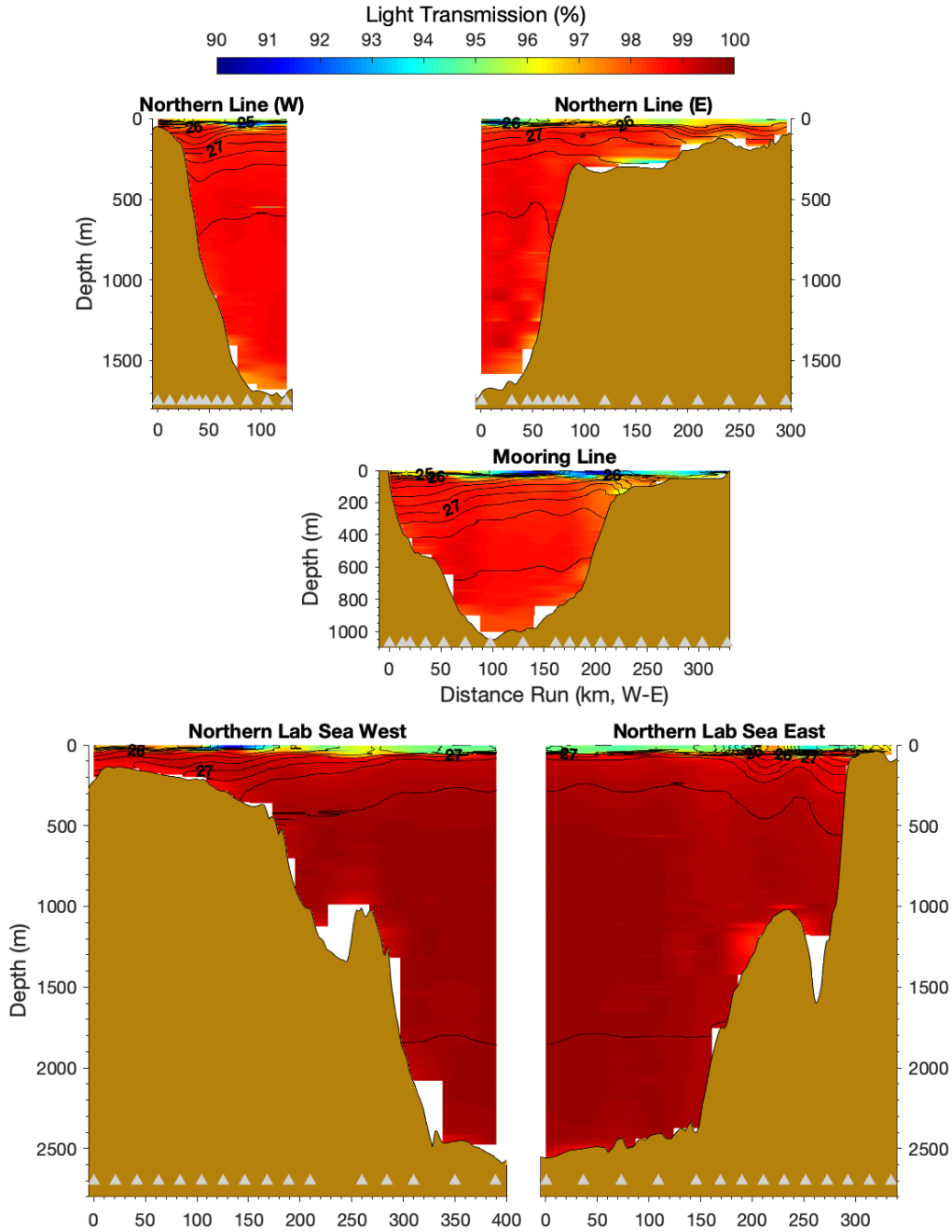


Figure 11a. Beam-c (% transmission) along the Northern, Mooring, and West/East Labrador Sea sections. Gray triangles mark station locations.

Davis Strait 2022 - Light Transmission (beam-c)

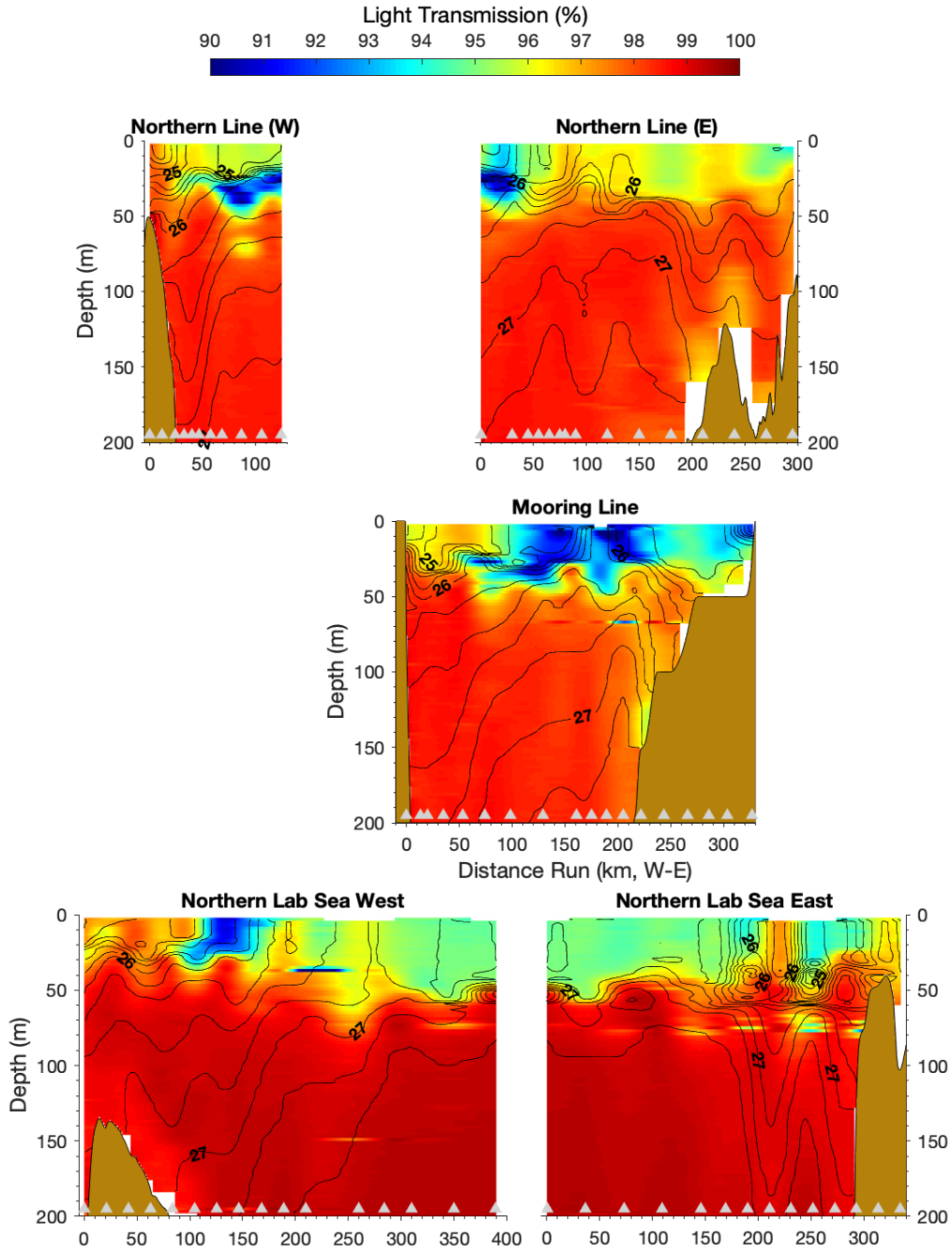


Figure 11b. Beam-c (% transmission) of the upper 200 m along the Northern, Mooring, and West/East Labrador Sea sections. Gray triangles mark station locations.

5. UNDERWAY SURFACE WATER pCO₂ AND TSG

R/V *Armstrong* is equipped with a General Oceanics pCO₂ system with NOAA standard gases and the Seabird SBE-45 thermosalinograph (TSG). The shipboard scientific services group (SSSG) of R/V *Armstrong* maintained both systems. During the rough seas on Sept. 30, Oct. 2, and Oct. 13, pCO₂ values showed many outliers due to bubble intrusion and measurements were suspended.

6. PHYTOPLANKTON AND PARTICULATE CARBON

The Greenland Institute of Natural Resources focused on quantifying phytoplankton biomass, diversity, community structure, and productivity. Measurements included photosynthetically available radiation (PAR), chlorophyll fluorescence, chlorophyll *a* concentration, oxygen respiration, particulate organic carbon (POC) and nitrogen (PON), and microscopy and DNA barcoding of samples for microbial community structure. Samples were collected along the Mooring Line (ML), Northern Line (NL) and the Labrador Sea sections (LSW and LSE) (**Fig. 2**). In addition, fjord transects were sampled in the Godthåbsfjord (GF) and the Ameralik fjord (AM) near Nuuk. The fjord transect stations are part of a time series of the Greenland Ecosystem Monitoring Program (GEM; www.g-e-m.dk) started in 2005.

7. ZOOPLANKTON

Zooplankton observations aim to understand the effect of environmental factors (temperature, salinity, oxygen, phytoplankton biomass, and size distribution) on zooplankton species composition, vertical distribution, and biomass. Special focus is on small zooplankton species of ≤ 1 mm in size, which are typically under-sampled by the standard WP2 nets that have a mesh size of 200 μm . These species dominate the zooplankton abundance in most places and times of the year and have been suggested to have become even more abundant due to climate change (*Balazy et al.*, 2018). The dominant small zooplankton species, *Oithona* spp., *Triconia* spp. and *Microsetella norvegica* do not feed on suspended phytoplankton but are known to feed on sinking particles (*Green & Dagg*, 1997), and therefore influence the attenuation of vertical flux (*Koski et al.*, 2020). The zooplankton work in Davis Strait contributes to our understanding of the role of these small zooplankton on the functioning of pelagic ecosystems and its potential climate-induced change.

The vertical distribution of zooplankton biomass and species composition were investigated using a Multinet Midi (Hydrobios). Zooplankton was sampled at five depth layers, using 50- μm nets.

8. SEABIRDS

Seabird surveys were conducted through a collaboration with the Canadian Wildlife Service (CWS), Environment and Climate Change Canada (ECCC), as part of the Eastern Canada Seabird Surveys at Sea (ECSAS) program, a long-term seabird monitoring program that identifies the distribution and behavior of seabirds at sea throughout the year. The survey data are used to identify and minimize the impacts of human activities on birds in the marine environment, and to track changes in distribution and abundance over time, which may reflect changes in ocean conditions, including those related to climate change. The ocean appears homogeneous at the surface, but seabird distribution is not random – it generally reflects the bathymetry and oceanographic conditions that are mostly invisible at the surface. Seabird surveys conducted in concert with biological, chemical, and physical oceanographic monitoring and research helps to explain the distribution of seabirds at sea. Conversely, seabird distribution can signal important oceanographic phenomena occurring below the surface.

Seabird surveys were conducted during transits between oceanographic stations along the transect lines in the Davis Strait and Labrador Sea from 30 September to 22 October 2022. Surveys were conducted while the ship was moving at speeds greater than 4 knots, looking forward and scanning a 90° arc to one side of the ship. All birds observed on the water within a 300 m-wide transect were recorded, and we used the snapshot approach for flying birds (intermittent sampling based on the speed of the ship) to avoid overestimating abundance of birds flying in and out of transect. Distance sampling methods were incorporated to address the variation in bird detectability. Marine mammal and other marine wildlife observations were also recorded, although surveys were not specifically designed to detect marine mammals. Details of the methods used can be found in the CWS standardized protocol for pelagic seabird surveys from moving platforms (*Gjerdrum et al.*, 2012).

9. PRELIMINARY RESULTS

Hydrographic Sections

Section plots for preliminary (uncalibrated) salinity, σ_t , oxygen saturation, beam attenuation, and pH along the ML, with T-S diagram using ML and NL observations are shown in **Fig. 12**. Four major water masses were observed along the ML: (1) the Arctic Water (AW, salinity <33.7 and temperature <0°C at the core) occupying the western side of the section to 300 m deep and extending to the Greenland Slope, (2) the West Greenland Shelf Water (WGSW, temperature >4°C, salinity <33.5) on the West Greenland Shelf with the front at ML10, (3) warmer and saltier West Greenland Irminger Water (WGIW, temperature >2°C, salinity >34.5) at the shelf break to 700 m deep along the West Greenland Slope, and (4) the Baffin Bay Deep Water (BBDW, temperature

$<2^{\circ}\text{C}$, salinity ~ 34.5 , $27.65 < \sigma_{\theta} < 27.72$) at the deepest part of the Strait. Oxygen saturation and pH show a similar distribution: highest at the surface water and decreasing with depth. Horizontal gradients reflect the water masses, with higher oxygen saturation and pH in the WGSW, while lower oxygen saturation and pH in the AW. Bottom nepheloid layers were observed at almost every station. Sources of materials (surface derived biogenic particles vs. land/glacier derived sediments) and physical control of these layers including isopycnal bottom currents, diapycnal turbidity currents, and internal waves need to be investigated.

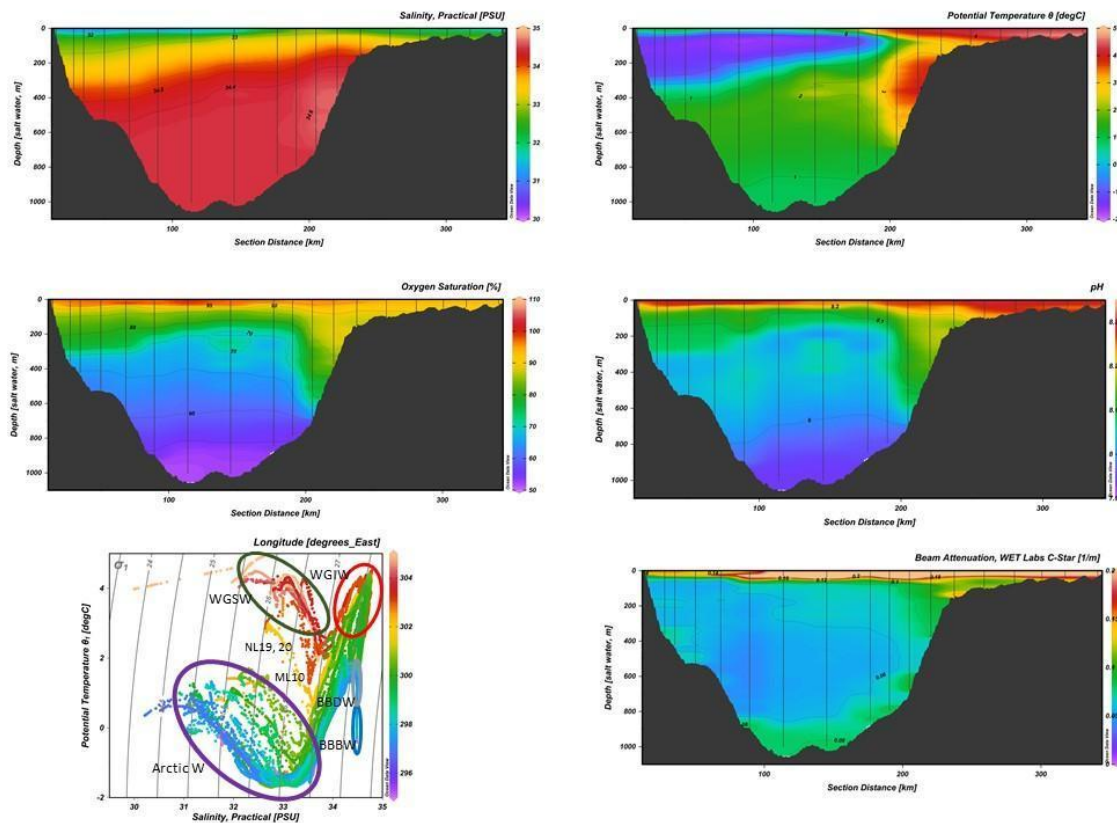


Figure 12. Salinity, temperature, oxygen saturation, pH, and beam attenuation along the ML.

Source and formation mechanisms of the Baffin Bay Bottom Water (BBBW) are not well understood. Although salinity, temperature, and density seem uniform at depths (Fig. 13), water masses below 2000 m show subtle differences, becoming colder, saltier and denser with lower oxygen saturation and higher beam attenuation (Fig. 14).

Homogeneity of this water mass and contrast with the water above may point to remote origins and horizontal advection to the site, with long residence times.

Baffin Bay Bottom Water (BBBW)

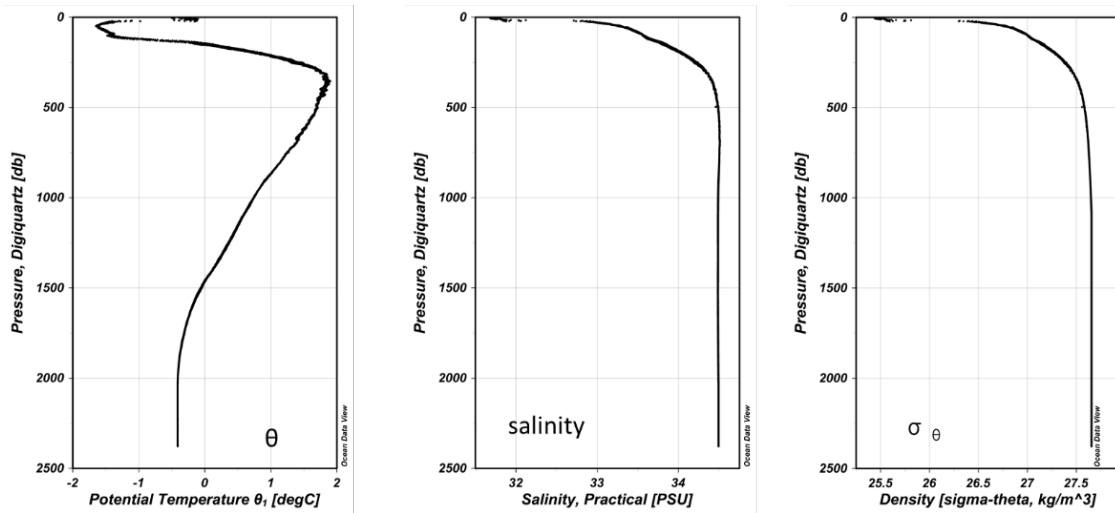


Figure 13. Temperature, salinity, and density at the BPR station.

Peculiar bottom layer with well-mixed salinity, θ and σ_θ below 2000m

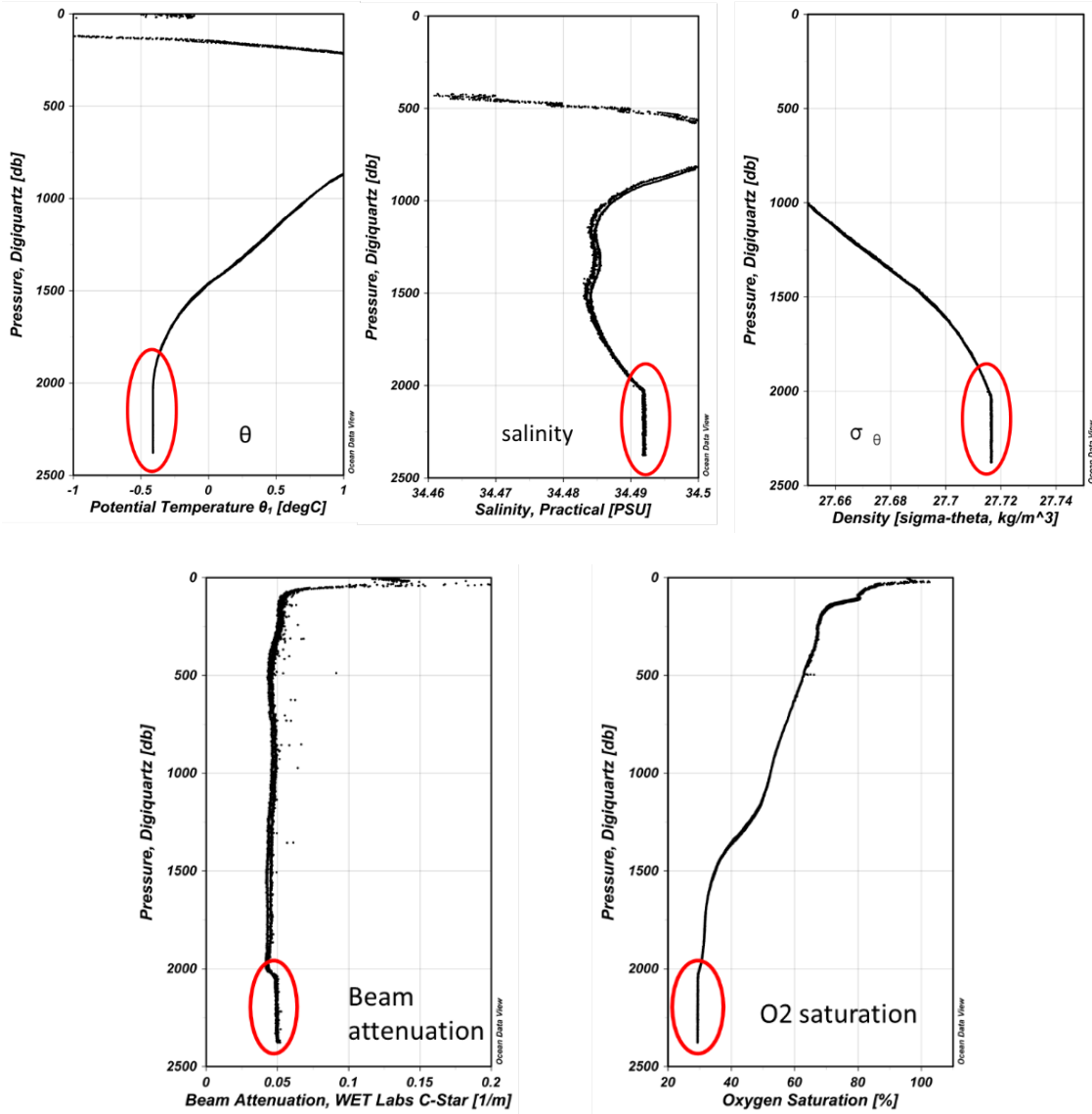


Figure 14. Salinity, temperature, σ_θ , beam attenuation, and oxygen saturation in the BBBW at the BPR station.

Dissolved Organic Matter (DOM)

Samples for analyses of dissolved organic matter (DOM) were collected to investigate the use of optical properties as a tracer of freshwater and organic carbon exported from the Arctic. These measurements complement previous work in the central Arctic Ocean, Fram Strait, and Davis Strait. To characterize the dissolved organic matter in the Davis Strait, seventy-nine 4-L water samples were collected at varying depths from the CTD rosette along the mooring line, at the bottom pressure recorder station, and in the fjord. Samples were stored immediately after collection, and were filtered on board using a 0.22- μm filter cartridge and peristaltic pump. Filtered samples were acidified to pH=2 using concentrated (12N) HCl in a fume hood. Acidified samples were used to perform solid phase extraction of dissolved organic matter onto preconditioned Agilent BondElut XAD resin cartridges. Extracted DOM samples will then be eluted in the lab after returning from the cruise and analyzed using Fourier-transform ion cyclotron resonance mass spectrometry.

Water sampling and laboratory processing

Water samples were collected to quantify three fractions of the DOM pool: dissolved inorganic carbon (DIC), colored dissolved organic matter (CDOM), and fluorescent dissolved organic matter (FDOM). A total of 460 samples were collected at 50 stations along the Mooring Line, Northern Line, BPR station, western and eastern Labrador Sea transects, and the Godthåbfjord transect. Water was collected from between 6 and 19 depths at each station depending on the local bottom depth. Water was collected directly from the Niskin bottles and filtered through a 0.3- μm glass fiber filter using a handheld syringe in the laboratory. The samples were then transferred into two 50-mL pre-combusted acid-washed glass vials. Half of the sample was acidified with Orthophosphoric acid (HPO) in preparation for DOC analysis. The other half was collected for CDOM and FDOM analyses. Both vials were stored cold at approximately 4°C.

In-situ CDOM sensor

A WetLabs fluorometer measuring CDOM at the 370/460-nm excitation/emission wavelength pair was mounted on the CTD package for the entire cruise. The acquired profiles provide a high-resolution complement to the water samples collected for DOM analyses.

Analyses

CDOM absorption spectra were measured onboard with a Shimadzu Spectrophotometer at 2-nm wavelength interval across the 200–800-nm wavelength range. Samples acclimated for one hour prior to analysis. Further analyses of the FDOM and DOC fractions will be conducted at DTU Aqua with a Horiba Aqualog Fluorescence Spectrophotometer and Shimadzu TOC-VCPH analyzer, respectively.

^{129}I , ^{236}U and ^{14}C as Transient Tracers of Ocean Circulation

The anthropogenic radionuclides ^{129}I and ^{236}U have been released to the ocean by anthropogenic nuclear activities such as bomb tests and the release from nuclear reprocessing plants in Sellafield (UK) and La Hague (France). The release from nuclear reprocessing plants is well documented, and labels northward flowing Atlantic waters. In the western subpolar north Atlantic, waters recirculating from higher latitudes such as the west Greenland current are labeled with the tracers and allow studies of the northward flow of Atlantic waters in the Labrador Sea and Davis Strait. Waters of Arctic/Pacific origin only carry the radionuclide signal from bomb tests and have a very different signature compared to the reprocessing plant signal. These differences allow studies of water mass origin, mixing processes, and timescales using these artificial radionuclides. In addition, the natural and artificial presence of the ventilation tracer ^{14}C can be used to add information about long vs. short term water mass circulation.

Our goal during the Davis Strait 2022 cruise is to study the time scales of the outflow of Arctic waters through Davis Strait, the evolution of the northward flowing Atlantic waters and the origin of deep and bottom waters using the radionuclides ^{129}I , ^{236}U , and ^{14}C as water mass tracers.

To disentangle the inflowing and outflowing water masses, we collected 165 samples of ^{129}I and ^{236}U along 11 depth profiles at the Mooring Line (ML 01, 03, 05, 07, 08, 10, 11, 12, 14, 16, 18), 10 depth profiles at the Northern Line (NL 01, 03, 05, 07, 09, 13, 15, 19, 23, 25), the BPR and JUNC station, and eight depth profiles in the Labrador Sea (LSW 07, 10, 12; LSE 03, 07, 10, 11, 13). We also collected surface and bottom samples in three stations at GF (03, 05, 08). For ^{14}C , samples were collected from several depth profiles at ML (03, 08, 16), NL (03, 09, 19), BPR, and JUNC.

Samples of ^{129}I were collected in 250-mL opaque plastic bottles, ^{236}U samples were collected in 3 L plastic cubitainers. ^{14}C was sampled in 100-mL borosilicate glass bottles, poisoned immediately using saturated mercury chloride solution (30 μL) and closed using rubber septa and aluminum caps.

At ETHZ, the ^{129}I and ^{236}U will be purified and extracted following the protocols described in *Castrillejo et al.* (2017), while the ^{14}C extraction and processing will be performed according to *Casacuberta et al.* (2020). The processed samples will be measured using accelerated mass spectroscopy at the Laboratory of Ion Beam Physics at ETHZ. To ensure high quality of the sample measurements, external and in-house standards as well as blanks and replica will be measured together with the samples. Results can be expected through late 2023.

Carbonate system/methane/nutrients/dissolved oxygen/oxygen isotope composition ($\delta^{18}\text{O-H}_2\text{O}$)/salinity/CTD/underway pCO₂/underway TSG

Sustained measurements of carbonate system parameters, methane, nutrients, oxygen, and oxygen isotopes at Davis Strait document changes in the interactions between the Arctic and North Atlantic subpolar gyre. As a gateway between the Arctic and the North Atlantic, quantification of the carbonate system and nutrients along Davis Strait contributes to understanding the global carbon cycle, the progress of ocean acidification and the propagation of changes in nutrient and oxygen dynamics, as well as freshwater composition characterized by oxygen isotopes, from the Arctic to lower latitudes.

Total Dissolved Inorganic Carbon (DIC) and Total Alkalinity (TA)

Seawater samples were collected in 500-mL borosilicate glass bottles for determination of total dissolved inorganic carbon (DIC) and total alkalinity (TA). Samples were preserved with mercuric chloride following SOP 1 in *Dickson et al.* (2007). Samples were kept at room temperature and transported by land from Woods Hole, USA to the Bedford Institute of Oceanography for analysis. In total, 537 samples were collected (**Table 8**).

Table 8. Samples collected/analyzed for/by Bedford Institute of Oceanography

	pCO ₂ /CH ₄	O ₂	DIC/TA	pH	$\delta^{18}\text{O}$	Salinity	nutrients
Mooring Line (ML)	78	54	153	153	187	36	382
Northern Line (NL)	15	45	139	139	160	30	310
Labrador Sea (LSW/LSE)	20	57	136	136	176	36	328
Bottom Pressure Rec (BPR)	19	8	19	19	20	2	38
Godthåbsfjord	28	19	61	61	61	10	164
Ameralik Fjord	12	12	29	29	1	10	42
Total Samples	132	195	537	537	605	124	1264

Spectrophotometric pH

537 samples for pH analysis were collected from the same Niskin bottles from which DIC/TA samples were collected. Samples were analyzed on board within 6 hours of sample collection. Water was collected in 200-mL borosilicate glass bottles, allowing each sample to overflow by at least one volume, allowing for a small headspace to

account for sample expansion upon subsequent warming. Samples were not preserved and were kept at 4°C until analysis.

Seawater pH was analyzed using the spectrophotometric method described in “Guide to best practices for ocean CO₂ measurements” SOP 6B (*Dickson et al.*, 2007). Bottles were then placed in a water bath held at 25 ± 0.05°C and allowed to thermally equilibrate for 30 minutes. The pH Apollo (AS-pH2) front-end prep system mixed 20 μL of the purified indicator dye *m*-cresol purple (University of South Florida) with the sample. The absorbance of light at the wavelengths 434 and 578 nm was measured using an Agilent model 8454 photodiode array spectrophotometer. Extinction coefficients at these wavelengths were used to determine the pH of the sample.

The performance of the spectrophotometer was monitored by daily measurements of Certified Reference Materials (batch # 196) from Scripps Oceanographic Institution. Precision was better than ± 0.001 pH units.

Some minor issues were experienced early in the cruise due to a faulty USB hub, which resulted in a loss of connection between the Agilent spectrophotometer and the computer, cancelling the run and compromising the sample integrity. Several samples were lost (5 in total), but this issue was fully resolved by NL12, cast 34.

Discrete pCO₂ and Methane

Water samples for pCO₂ and methane measurements (they are measured from the same bottle) were collected drawn from the rosette into 160-mL volume vials, allowing each sample vial to overflow by about 3 volumes before immediate preservation with 50 μL of saturated mercuric chloride solution prior to sealing with crimp seal caps and butyl rubber septa. 133 samples were collected in total (**Table 8**).

Since sampling for fjords were not originally planned, we didn't have sample bottles. To collect samples in the fjords, we replaced some samples from NL and NLS samples with fjord samples. The samples were stored at 4°C in a refrigerator until demobilization in Woods Hole, Massachusetts, then transported to BIO for analysis by static headspace equilibrium gas chromatography using an GC-FID equipped with a catalytic methanizer.

δ¹⁸O-H₂O

Samples for stable isotope δ¹⁸O-H₂O analysis were collected in 60-mL Boston amber round bottles with air-tight phenolic caps. 605 samples were collected in total (**Table 8**). The samples will be analysed by isotope ratio mass spectrometry (IRMS) at the Jan Veizer Isotope Lab, University of Ottawa.

Dissolved Oxygen

195 dissolved oxygen samples were collected and measured using the Winkler titration method on board, following the GO-SHIP protocol by *Langdon* (2010). These measurements were conducted to calibrate an oxygen sensor on the CTD. In most stations, samples were collected at 10 m, at the chlorophyll fluorescence maximum, and at the bottom.

Some issues with dissolved oxygen (DO) analysis occurred along the ML starting with ML12 (cast 2), until NL 05 (cast 43). Many of these DO samples were compromised due to two issues: first, intermittent issues with reagent dispenser for the Winkler II (alkaline iodide) affected reagent delivery, which resulted in poor precipitate formation and the titration sometimes did not proceed correctly. This was resolved with a new dispenser. Secondly, samples were lost due to bubble formation from the sample on the lens. Typically, samples are warmed up to room temperature prior to analysis, but a satisfactory alternate method at 4°C was employed following testing at room temperature and at 4°C to confirm accuracy. For the rest of the cruise, DO samples were kept at 4°C until immediate analysis. Some of this DO data are recoverable using the BOB software to perform endpoint recalculation.

Salinity

124 samples were collected in 200-mL borosilicate glass bottles to calibrate CTD salinity. Samples were kept in room temperature and will be measured using a Guildline Autosol salinometer at Bedford Institute of Oceanography following the GO-Ship protocol by *Kawano* (2010). In most stations, samples were collected at 5 m and from the bottom.

Nutrients

Duplicate of 632 samples (total of 1264 samples, **Table 8**) were collected in acid washed 10 mL sample tubes and kept frozen at –80°C on board due to the availability of the freezer space. Samples were kept frozen with dry ice during transport from Woods Hole to Bedford Institute of Oceanography and transferred to the freezer (–20°C) till analysis.

Underway Surface pCO₂

The pCO₂ distribution is similar to that of temperature and salinity in general, higher at the Greenland coast than Baffin Island coast (Fig. 15). When the wind was strong and

mixed the surface water, deeper CO_2 were transported to the surface and elevated CO_2 was observed, for example on October 1 (66.9°N , 56.1°W) and October 18 (63.2°N , 60.6°W). With the exception of these stormy periods, surface pCO_2 were much less than $400 \mu\text{atm}$ and the region is a strong sink for the atmospheric CO_2 during the study period.

Two fjords near Nuuk were studied during the last two days of the cruise. These two fjords were sampled regularly by scientists at Greenland Institute of Natural Resources. However, this is the first time that fjords were studied by a group of scientists with different expertise. Higher spatial variations observed with underway systems showed the strong contrast between two fjords with tidewater glaciers (Godthåbsfjord) and a land-terminated glacier (Ameralik Fjord) (**Fig. 16**). Surface waters in Godthåbsfjord are colder and fresher than that in Ameralik Fjord. Surface pCO_2 in Godthåbsfjord is extremely low which indicates a strong sink of atmospheric CO_2 in this fjord. Ameralik Fjord also shows the strong sink of atmospheric CO_2 , however, higher pCO_2 was observed than Godthåbsfjord. Higher fluorescence in Godthåbsfjord may indicate the higher biological uptake of CO_2 , and contribute to the observed low pCO_2 . The effects of temperature, salinity, and biological uptake to pCO_2 need to be evaluated separately. As many glaciers retreating in Greenland, the contrasting biogeochemical properties in these adjacent fjords may provide an interesting analogue of future fjord systems and their consequences in carbon uptake and marine ecosystems.

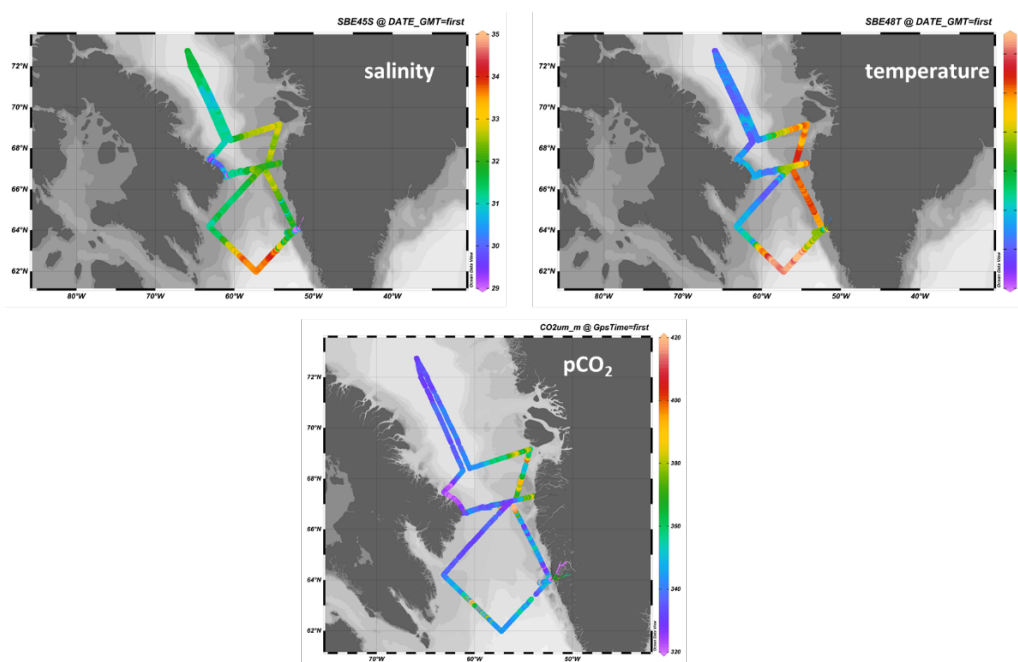


Figure 15. Surface (5 m) underway measurements of salinity, temperature, and pCO_2 .

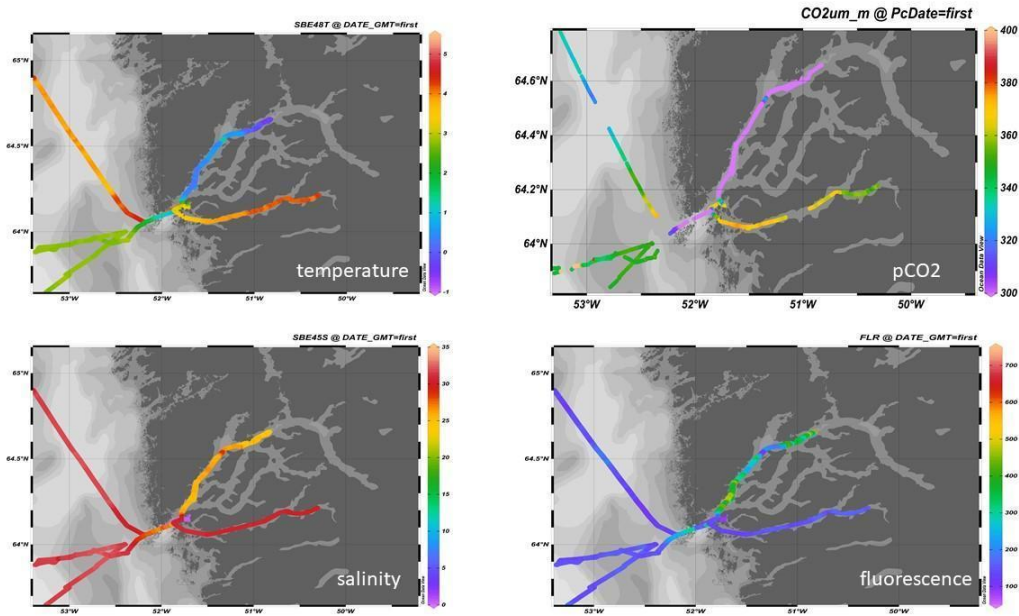


Figure 16. Underway (5 m) temperature, salinity, pCO_2 , and fluorescence in Godthåbsfjord and Ameralik Fjord.

Shipboard Conditions and Problems

Major problems of the cruise arose from the shipping. Some chemicals shipped from Canada and Switzerland didn't arrive on time for the departure of the vessel. With the help of GINR scientists, we managed to avert major problems, but we need to evaluate the shipping time as well as the costs, which became extremely expensive, in future. Difficulty in communication (no response) with shipping agents resulted in uncertainties and stress of operations.

Due to the rough weather at the beginning of the cruise, the plans for mooring and hydrography needed to be modified. Because we had 12-hour shifts (noon-midnight and midnight-noon), it was difficult to adjust the shift schedule when occupying different lines. We recommend day and night shifts (6 am to 6 pm and 6 pm to 6 am) for the next operation.

We grossly underestimated the number of Niskin bottles fired in this cruise and consequently ran out of ID labels (stickers). A new numbering system, starting at 001, was applied at the LSW11. Additionally, the sampling protocol for different parameters

were not established well at the beginning of the cruise and this occasionally caused a shortage of sampling water for biologists who sampled last from the Niskin.

Closer evaluation of the storage space is required for the next cruise. The walk-in freezer of R/V *Armstrong* could not be cooler than -15°C , which made it difficult to store nutrient samples that need to be maintained below -20°C . Also, the science hold is difficult to access with heavy glass bottles filled with samples. Better space management is required.

For many early career scientists, this was the first experience on an offshore cruise. They worked hard and learned various tasks very quickly. Many discussions on board were delightful. The support of SSSG (Emily Cheung and Sonia Brugger) was fantastic and we owe the success of this cruise to them.

Phytoplankton and Particulate Carbon

Upwelling driven by northerly or southerly winds along the coasts can drive high phytoplankton production and biomass near the shelf breaks. Because the Greenland shelf slope is influenced by nutrient-rich Atlantic water masses and the Canadian shelf slope by nutrient-poor Arctic water masses, upwelling on the Greenland side is expected to have the strongest fertilization effect. Inshore, Godthåbsfjord is influenced by tidewater glaciers, and subglacial upwelling has been described as an important mechanism for nutrient upwelling into the euphotic zone, fueling summer and autumn primary production. Ameralik fjord is only fed by input from a land-terminating glacier and lacks this subglacial upwelling effect. Thus, we expected higher phytoplankton biomass and production in GF.

Phytoplankton primary production was estimated via photosynthesis-irradiance (PI) curves using a pulse amplitude modulated fluorometer (PAM). The PAM estimates electron transport rates (ETR) in the photosystem based on the increase in chlorophyll fluorescence after pulses of different light intensities. The PI curves give direct information about the communities' maximum potential ETR (ETR_{max}), their overall fitness (F_v/F_m), and their efficiency to use low light intensities (α). In addition, the data can be used to model primary production in the water column using the *in situ* PAR profiles from the CTD or manual measurement, and chlorophyll profiles measured by the GINR during the cruise. PI curves were measured at all 75 stations with water samples from all depths down to 50 m unless noted otherwise (**Tables 4–7**).

The PI curve parameters show high phytoplankton fitness ($F_v/F_m > 0.6$) and efficient and high potential photosynthesis (α , ETR_{max}) at all stations. As hypothesized above, the maximum potential photosynthesis (ETR_{max}) is lowest in the deeper basins and increases towards the shelf breaks (**Fig. 17**). In the Labrador Sea transect the highest ETR_{max} is found on the Greenland side, whereas the highest ETR_{max} values in the Baffin

Bay ML and NL transects are found near the Canadian shelf break (**Fig. 17**). Inside both fjords ETR_{max} stays at values similar to the Greenland shelf. The initial slope of the PI curve (α) is highest at the Greenland shelf break in the Labrador Sea (LS transect) and in the fjords, while the values in the Baffin Bay transect are lower and more homogeneous. Both fjords have α values comparable to the shelf. Surprisingly, α in the Ameralik fjord continues to increase towards the inner part of the fjord reaching values exceeding GF despite the lack of tidewater glaciers. The increasing α is likely a result of increasing silt concentrations (turbidity), which necessitates increasing low light adaptation (higher α).

Microbial community respiration was estimated in oxygen respiration vials (PyroScience Firesting system). At 61 stations 20-mL water samples from 5 m, 20 m, the chlorophyll maximum, and the bottom were incubated at 3°C for at least 2–3 h in respiration vials. Via oxygen-dependent quenching of a fluorescent film inside the vials, oxygen was measured continuously in 1-s intervals. Oxygen depletion in the linear phase of the profiles will be used to calculate respiration rates. The Winkler based oxygen measurements will be used to calibrate the oxygen sensors and correct the measurements for potential drift.

The microbial community structure will be characterized via a) microscopy of Lugol-fixed phytoplankton water samples and b) DNA metabarcoding of filtered water samples. For DNA metabarcoding 1.5-L water samples from 5 m and the chlorophyll maximum were filtered from 29 stations at 3°C onto Sterivex filters using a peristaltic pump. Later the DNA will be extracted and part of the 16S rRNA (bacteria and archaea) and 18S rRNA (eukaryotes) genes will be sequenced.

Phytoplankton biomass was estimated using chlorophyll *a* measurements and *in situ* fluorescence measurements on the CTD. Fluorescence measurements of the CTD will later be calibrated using the measured chlorophyll *a* value. Total chlorophyll *a* concentration (GF/F; 0.7- μ m size fraction) was measured filtering 300 ml of sea water from 9 depths in the upper 100 m in triplicate on all water stations. Filters were extracted in 96% ethanol (24 h in dark) or frozen at -20°C until fluorometric analysis (Turner Trilogy Fluorometer). On Biology/Full stations >10 μ m chlorophyll *a* concentration was measured at all depths to estimate the phytoplankton biomass available to larger copepods. A preliminary analysis of CTD fluorescence profiles shows that only a fraction of the biomass is in the upper 10 m and that integration over the entire euphotic zone is necessary to get an accurate estimate of the integrated biomass (**Fig. 18**). The highest integrated biomass has been measured at some distance from the Canadian shelf break on all offshore transects. Only the LS transects show a similar increase near the Greenland shelf break. While surface chlorophyll *a* concentrations were relatively high in the fjords, the integrated biomass was substantially lower than in the offshore transects, with a sharp decreasing trend into the fjord. Surprisingly, Ameralik Fjord, the fjord lacking a tidewater glacier, has overall higher integrated chlorophyll *a* biomass compared to the tidewater glacier influenced GF.

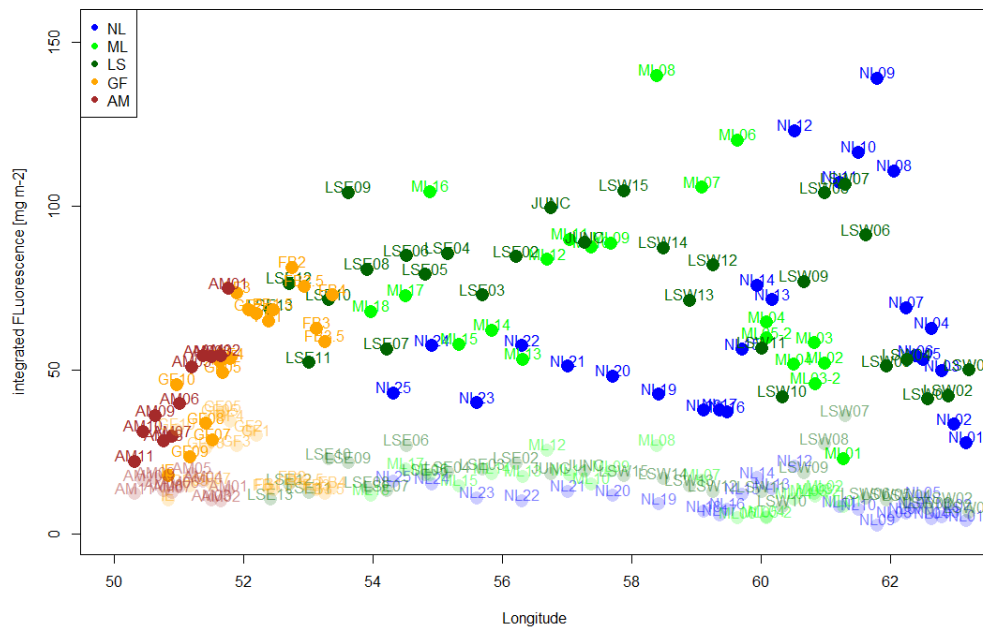


Figure 18. Preliminary results of the integrated chlorophyll fluorescence measured with the CTD. Transparent colors indicate integrated values over 10 m, while the full colors show the integrated fluorescence over the entire euphotic zone.

Particulate organic carbon (POC) and nitrogen (PON) were sampled at all stations at 50, 100, 500, 1000 m and at the depth of near bottom and maximum chlorophyll *a*. Sea water (5 L) from each depth was filtered onto 47-mm precombusted (450°C for 5 h) GF/F filters (0.7 μm) and frozen at -20°C . Swimmers are removed before they are dried (60°C for 24 h) and analyzed on either a CHN elemental analyzer or mass spectrometer.

Zooplankton Biomass and Vertical Distribution

Multinet samples were taken on the “full stations” (biological sampling stations; **Table 9**). Due to technical issues with running the multinet in offline mode, the sampling of NL17 and NL19 was not conducted, and the sampling of stations ML05 and LSW03 had to be skipped due to bad weather. Due to the breakage of the nets on stations ML02 and ML03, the data collection of later stations consists only of three depth layers. The samples will be analyzed in the spring of 2023, when the abundance and biomass of species will be determined.

Table 9. Stations, dates, time, and sampling depth of multinet samples.

Sample no.	Station	Longitude (W)	Latitude (N)	Date	Time	Net	Depth
	ML01	61.241159	66.659271	12 Oct 2022	15:30	Max depth	69
						Activation depth	55 (T: 62)
1						1	50-40
2						2	40-30
3						3	30-20
4						4	20-10
5						5	10-0
	ML02	60.969587	66.671314	12 Oct 2022	17:27	Max depth	378
						Activation depth	355 (T:370)
7						2	200-100
8						3	100-50
9						4	50-10
10						5	10-0
	ML03	60.759579	66.685699	12 Oct 2022	22:51	Max depth	438
						Activation depth	410 (T:430)
11						1	400-200
13						3	100-50
15						5	10-0
	ML08	58.375251	66.929977	13 Oct 2022	21:04	Max depth	1035
						Activation depth	930 (T:950)
23						3	900-100
24						4	100-50
25						5	50-0
	ML11	57.038142	67.034813	14 Oct 2022	03:54	Max depth	686
						Activation depth	630 (T:650)
28						3	600-100
29						4	100-50
30						5	50-0
	ML12	56.675517	67.067892	14 Oct 2022	05:41	Max depth	394
						Activation depth	330 (T:350)

33						3	300-100
34						4	100-50
35						5	50-0
	ML13	55.621733	67.167449	14 Oct 2022	22:50	Max depth	156
						Activation depth	135 (T:145)
38						3	120-50
39						4	50-10
40						5	10-0
	ML17	54.476836	67.265096	14 Oct 2022	19:47	Max depth	56
						Activation depth	45 (T:52)
43						3	30-20
44						4	20-10
45						5	10-0
	NL03	62.770328	67.624955	12 Oct 2022	04:22	Max depth	135
						Activation depth	110 (T:125)
46						1	100-50
47						2	50-30
48						3	30-20
49						4	20-10
50						5	10-0
	NL09	61.771534	68.047932	12 Oct 2022	15:55	Max depth	1692
						Activation depth	1520
51						1	1500-1000
52						2	1000-500
53						3	500-100
54						4	100-50
55						5	50-0
	LSW03	62.559517	63.959644	16 Oct 2022	05:13	Max depth	158
						Activation depth	140 (T:150)
57						3	125-50
58						4	50-10
59						5	10-0
	LSE01	56.740237	62.201145	18 Oct 2022	04:17	Max depth	2553
						Activation depth	2480 (T:2510)

67						3	2450-500
68						4	500-100
69						5	100-0
	LSE10	53.015395	63.749841	18 Oct 2022	10:08	Max depth	146
						Activation depth	120 (T:130)
72						3	105-50
73						4	50-10
74						5	10-0
	GF03	-51.881682	64.118427	20 Oct 2022	05:37	Max depth	350
						Activation depth	330 (T:340)
75						3	300-100
76						4	100-50
77						5	50-0
	GF07	-51.508863	64.425631	20 Oct 2022	16:45	Max depth	614
						Activation depth	580 (T:600)
78						3	550-100
79						4	100-50
80						5	50-0
	GF IE	-50.872117	64.647059	20 Oct 2022	22:33	Max depth	555
						Activation depth	530 (T:540)
81						3	500-100
82						4	100-50
83						5	50-0
Ring net samples							
BPR 500-0	BPR	-65.292745	72.745059	10 Oct 2022	01:30		500-0
BPR 50-0	BPR	-65.230041	72.745007	10 Oct 2022	01:51		50-0
GF3 100-0	GF3	-51.881682	64.118.427	20 Oct 2022	05:36		100-0

Seabirds

We conducted 1091 seabird surveys along 1614 km of ocean track over 21 days between 30 Sept and 22 October 2022 (**Fig. 19**). A total of 2100 individuals (21 species) were observed in transect (5080 sightings in total) from nine families (**Table 10**). Bird density averaged 3.8 birds/km² (range 0–355.0 birds/km²).

The most abundant bird species observed was the Northern Fulmar, a circumpolar breeder that feeds over deep waters and is known to follow ships in the hopes of securing an opportunistic feeding opportunity (**Figure 20a**). Other Procellariidae observed included both the Great and Sooty Shearwaters, which were sighted along the Labrador Sea west line (**Figure 20b**). These observations were unexpected as these species do not typically occur this far north, especially so late in the year. Both shearwater species breed in the Southern Hemisphere, and are abundant in the North Atlantic between April and September.

Black-legged Kittiwake were also abundant during surveys and made up 30% of the sightings in transect (**Table 10, Fig. 21**). This species breeds in colonies on cliffs in the North Pacific, North Atlantic, and Arctic oceans, feeding primarily on fish over the open ocean. Individuals observed during this survey were most likely from colonies in the eastern North Atlantic, and were traveling across Baffin Bay to their wintering grounds in Canadian waters. Other gull species observed during surveys included the Great Black-backed, Herring, Glaucous, and Iceland Gull, all of which breed in Arctic and sub-Arctic colonies throughout the region.

Dovekie made up a total of 16% of the observations (**Table 10**) and were observed in highest densities northwest of Nuuk and in the middle of Baffin Bay (**Figure 22a**). It is worth noting that the program was conducted a few weeks later than previous surveys. This may be the reason relatively few dovekie – an arctic seabird that breeds in the millions in the Thule region of northwest Greenland – were observed compared to previous surveys of the area. The peak of the Dovekie migration to the western North Atlantic had likely passed. The Dovekie is the only North Atlantic marine bird species that feeds almost exclusively on zooplankton (primarily *Calanus* copepods) and may serve as a good indicator of areas of high *Calanus* density. Other Alcids observed (all primarily piscivorous) include the Razorbill, Atlantic Puffin, Black Guillemot, and Thick-billed Murre (**Table 10; Fig. 22b**).

Table 10. Total number of each species observed during the ECSAS seabird surveys.

Family	English	Latin	Number sighted within transect	Total number sighted
Procellariidae	Northern Fulmar	<i>Fulmarus glacialis</i>	652	2542
	Great Shearwater	<i>Ardenna gravis</i>	23	51
	Sooty Shearwater	<i>Ardenna griseus</i>	32	47
Anatidae	King Eider	<i>Somateria spectabilis</i>	41	111
	Common Eider	<i>Somateria mollissima</i>	19	72
	Unidentified Eider	<i>Somateria</i>	0	2
Accipitridae	Peregrine Falcon	<i>Falco peregrinus</i>	0	1
Scolopacidae	Purple Sandpiper	<i>Calidris maritima</i>	0	3
Laridae	Pomarine Jaeger	<i>Stercorarius pomarinus</i>	7	10
	Great Black-backed Gull	<i>Larus marinus</i>	32	38
	Herring Gull	<i>Larus argentatus</i>	0	1
	Glaucous Gull	<i>Larus hyperboreus</i>	179	491
	Iceland Gull	<i>Larus glaucooides</i>	32	48
	Black-legged Kittiwake	<i>Rissa tridactyla</i>	635	880
	Unidentified gulls	<i>Larus</i>	0	21
Alcidae	Dovekie	<i>Alle alle</i>	339	514
	Razorbill	<i>Alca torda</i>	3	3
	Atlantic Puffin	<i>Fratercula arctica</i>	8	8
	Black Guillemot	<i>Cepphus grylle</i>	1	2
	Thick-billed Murre	<i>Uria lomvia</i>	93	188
	Unidentified Alcids	Alcidae	3	36
Corvidae	Common Raven	<i>Corvus corax</i>	1	1
Turdidae	Northern Wheatear	<i>Oenanthe oenanthe</i>	0	1
Emberizidae	Snow Bunting	<i>Plectrophenax nivalis</i>	0	9
Total			2100	5080

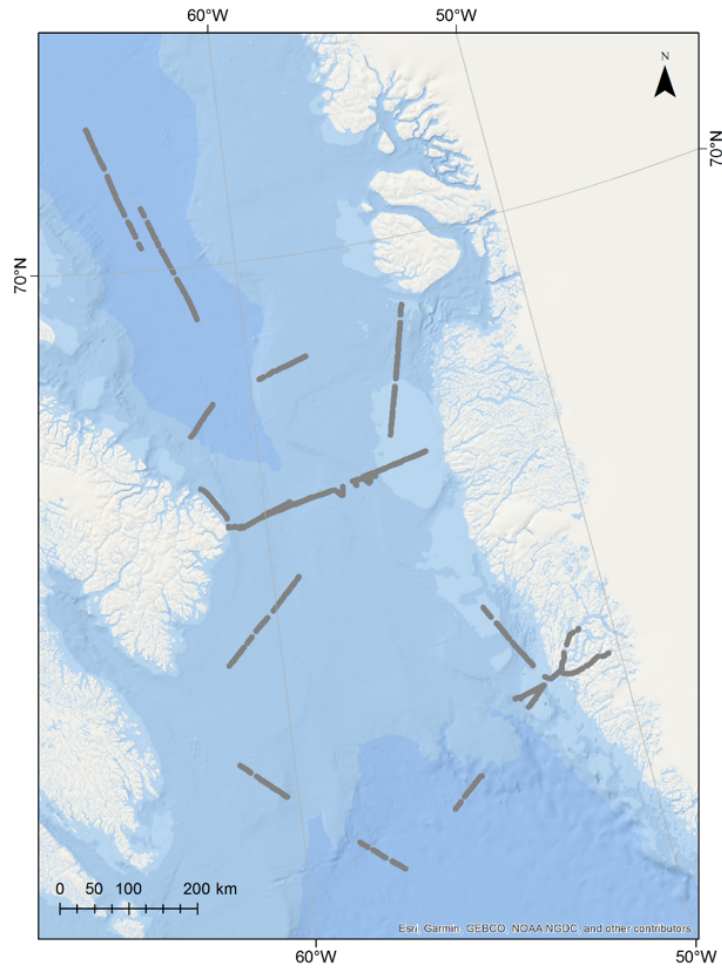


Figure 19. Location of ECSAS seabird surveys conducted during Davis Strait Gateway project from 30 September to 22 October 2022.

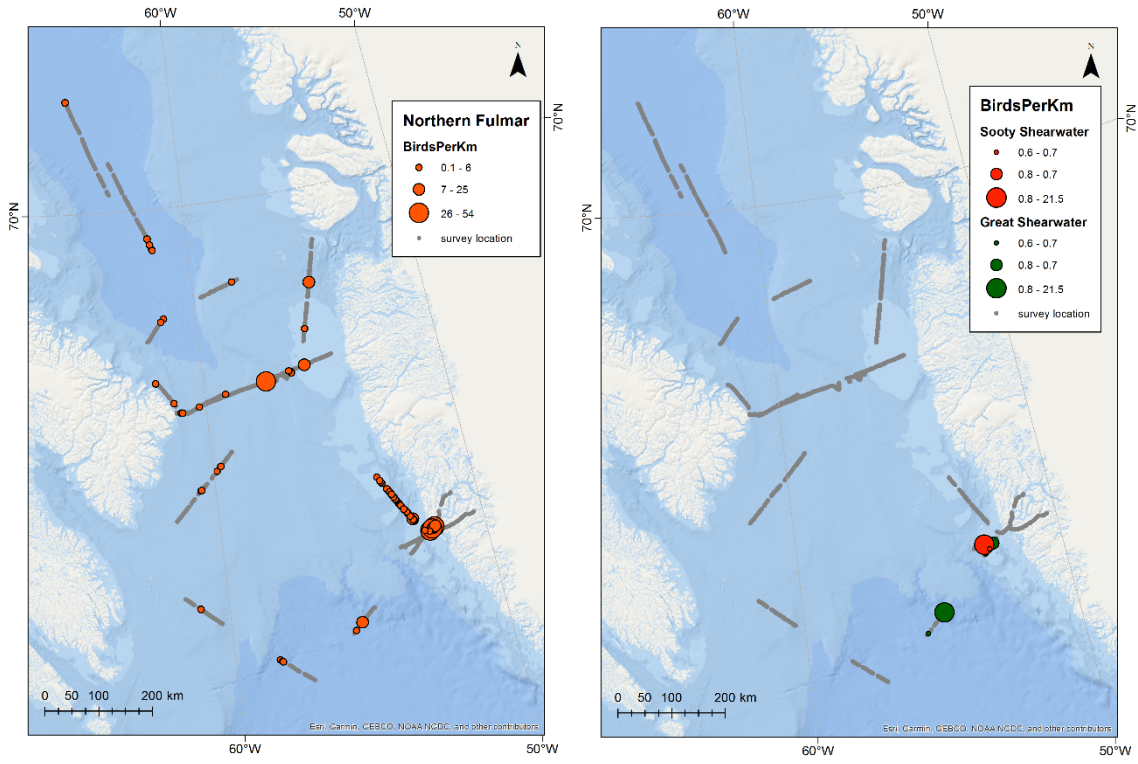


Figure 20. Linear density (birds/km) of (left) Northern Fulmar and (right) Great and Sooty Shearwater observed in transect during Davis Strait Gateway project from 30 September to 22 October 2022.

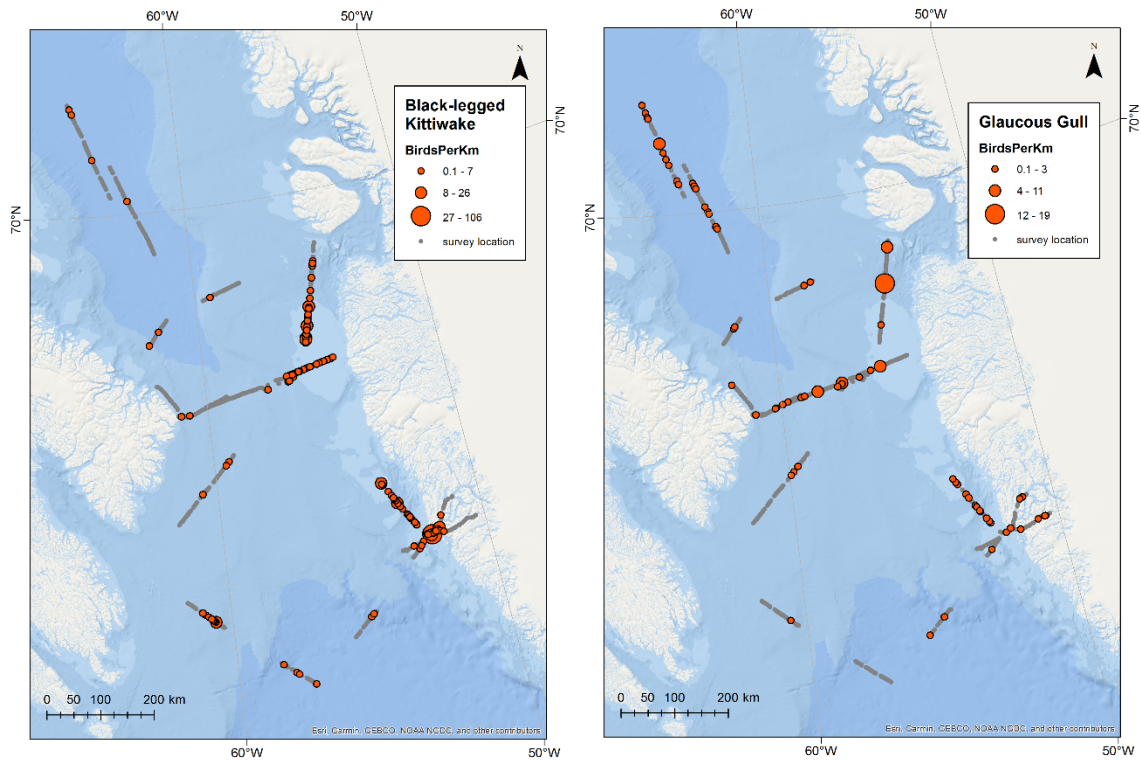


Figure 21. Linear density (birds/km) of (left) Black-legged Kittiwake and (right) Glaucous Gull observed in transect during Davis Strait Gateway project from 30 September to 22 October 2022.

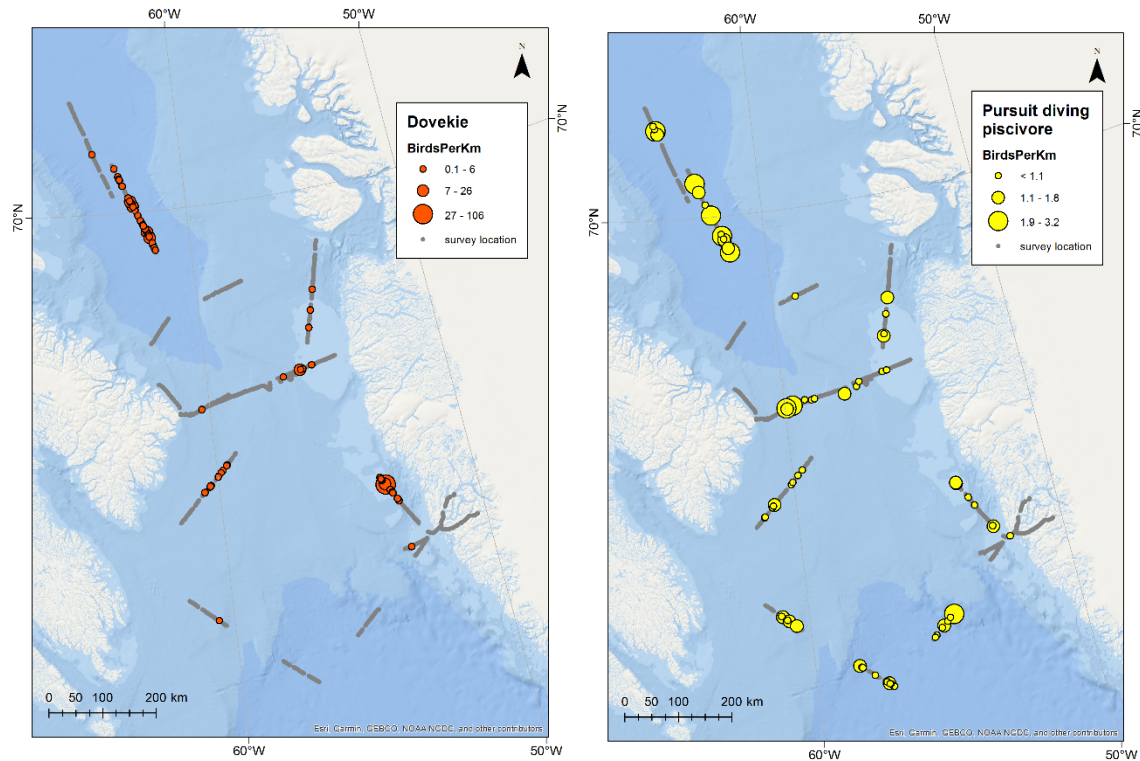


Figure 22. Linear density (birds/km) of (left) Dovekie and (right) diving piscivores including Razorbill, Atlantic Puffin, Black Guillemot, and Thick-billed Murre observed in transect during Davis Strait Gateway project from 30 September to 22 October 2022.

Autonomous and In Situ Water Sampling

Background

The National Oceanography Centre's involvement in the cruise related to the deployment of two remote autonomous water samplers (RAS) at the western boundary of the Davis Strait mooring line, and the collection of water samples across the mooring line transect to be analyzed for barium (Ba), rare earth elements (REE), neodymium, dissolved organic nitrogen and dissolved organic phosphate when back on land.

This work is part of the UK Natural Environment Research Council BIOPOLE (Biogeochemical processes and ecosystem functioning in changing polar systems and their global impacts, <https://biopole.ac.uk>) project. While BIOPOLE as a whole seeks to investigate how nutrients in polar waters (both north and south) drive the global carbon cycle and primary productivity, at Davis Strait specifically our intention is to interrogate the transport of nutrients from the Arctic into the subpolar North Atlantic. The Arctic

Ocean is a significant source of macro- and micronutrients to the North Atlantic, and the biological activity that ensues and the ecosystems that are supported there are typically determined by the unique chemical mixture signatures carried by water masses arriving in the region.

We hope to collect water samples every ~2 weeks in the core of waters that have moved across the Arctic Ocean from the Pacific. From analyses of inorganic (N, P, Si) and organic (N, P) nutrients we hope to determine a high resolution time series of nitrogen:phosphate stoichiometry export fluxes. Additional observations of nutrient sources upstream will then enable the determination of the dominant controls on the excess quantities of phosphate (in comparison to nitrogen) leaving the Arctic. Further water samples across Davis Strait were collected for the later analysis of Ba, REE, and Nd (and organic nutrients); the former have increasingly been utilized as water mass tracers of terrestrial-derived freshwater input (e.g., *Paffrath et al.*, 2021) — in the Arctic region, rivers draining from the Eurasian continent have been found to carry concentrations significantly different from those from North America. Combining with the mooring-based analyses will allow the assessment of the contribution of melting polar ice to the nutrient export and enable the quantification of the transport of nutrients southwards, their elemental stoichiometry and how they change seasonally and over time. Together it is hoped these will enable a step-change in our understanding in what drives biogeochemical variability, and how it is responding to human-derived pressures.

Remote Access Samplers (RAS)

The McLane Research Laboratories Inc. (www.mclane.com) Remote Access Sampler (RAS) 3-48-500 is an instrument for the autonomous collection of seawater samples (**Fig. 23**). It works by pumping water out of the bottom of an acrylic sample cylinder in which an evacuated sample bag is installed. A pressure gradient is created, and the removed volume is replaced by local seawater being pushed into the sample inlet, through a multi-position valve and into the bag. A movement of the valve back to its home position isolates the sample collected until recovery. Pre-injection of a sample preservative into the bag can mean the sample can be stored safely on the instrument indefinitely without compromising sample integrity. The sampler is capable of collecting 48, 500-mL samples, from a frequency of 3 samples an hour to a deployment period of 24 months.



Figure 23. RAS ready for deployment at C2.

Two RAS were co-deployed with Sea-Bird SBE37SMP MicroCATs (to measure temperature, pressure, and salinity) across the Davis Strait mooring line during AR69-04 (**Table 11**). Both instruments were configured in the same way. The first samples should be collected immediately after deployment, then subsequent samples every 16 days (**Table 12**). Samples collected from the corresponding CTD during the initial occupation of the mooring line transect (and from CTDs collected prior to recovery in 2024) will be used to help calibrate the outputs. All sampling events will start at 16:00:01 UTC, 14:00:01 local. RAS unit 14520-01 was deployed at C1 on 13 October 2022 and RAS unit 14520-02 was deployed at C2 on 14 October 2022. The NOC standard operating procedure for RAS deployment (*Brown and Rayner, 2015*) was followed during the instrumental setup for both RAS deployed as part of this trip.

- RAS time and date was set to UTC. Local time was UTC-2.
- Due to the ‘acid wash’ blue tubing becoming detached during a previous deployment, the position of this bottle was switched with that of bottle 48. This was to give it more protection towards the center of the RAS.
- The ‘acid wash’ bag was filled with artificial seawater preserved with mercuric chloride. A post-sample wash of 10 mL was programmed.

- A stainless-steel mesh was added to the top of each RAS with cable ties. This was to protect somewhat the sample inlet and tubing below from the chain and mooring fixtures above.
- 40% saturation mercuric chloride was used for the sample lines (approx. 1 mL volume each). Prior to addition its salinity was changed to as close as possible to local through the addition of NaCl.
- Instead of deionised water being used to fill the acrylic tubes, artificial seawater with a target salinity of 34 g/kg was used.
- Instrumental setup followed a set procedure: (pump primed, top line filled, bottom lines prefilled by reverse pumping, bags added, mercuric chloride added to sample lines and attached to bottle caps/valve, bags opened, acrylic cylinders filled, compensation tubes added, and programmed).
- Two types of bags were used: Tedlar (~650 mL, no bag valve) and Altef (~3 L, bag valve). Tedlar are known to interfere with the carbonate chemistry of collected samples through the interaction of a manufacturing impurity (dimethyl acrylamide, DMAC) with the water, whereas Altef bags do not suffer from the same problem.
- Bags were alternated in sample bottles, so a Tedlar bag would be followed by an Altef, and vice-versa. This allows the potential exploration of a monthly carbon time series from each sampler. The 3 L bags required the removal of excess plastic from their edges and folding in order for them to fit inside the acrylic cylinders.
- MicroCATs were added to the bottom of each RAS frame, at the opposite side to where the pump exhaust exited.

Discrete samples were collected on a number CTD stations for the later land-based analysis of barium, rare earth elements, neodymium, dissolved organic nitrate and dissolved organic phosphate.

In total, 10 CTD casts across 8 stations were sampled for chemical parameters (**Table 13**). Not all parameters were sampled for on all stations listed below. The methods followed for sample collection are as described in the GEOTRACES cookbook (2017). Ba, REE, and Nd were acidified by addition of 0.1% v/v trace-metal-free hydrochloric acid before being kept at lab temperature. Nutrient samples were immediately frozen for storage.

Table 11. Deployment details for Remote Access Samplers

	Mooring	
	C1	C2
Latitude	66.642 N	66.763 N
Longitude	60.775 W	60.078 W
Nominal depth	100 m	100 m
RAS Serial Number	14520-01	14520-02
RAS colour code	Yellow	Red
Sampling frequency	16 days	16 days
MicroCAT serial number	9394	9393
Sampling frequency	Hourly	Hourly

Table 12. Sampling schedule for barium, rare earth elements, neodymium, dissolved organic nitrate, and dissolved organic phosphate.

Sampling event / valve port	Date	Sampling event / valve port	Date
1	13 ⁺ Oct 2022 (C1) 14 ⁺ Oct 2022 (C2)	25	01-Nov-2023
2	29-Oct-2022	26	17-Nov-2023
3	14-Nov-2022	27	03-Dec-2023
4	30-Nov-2022	28	19-Dec-2023
5	16-Dec-2022	29	04-Jan-2024
6	01-Jan-2023	30	20-Jan-2024
7	17-Jan-2023	31	05-Feb-2024
8	02-Feb-2023	32	21-Feb-2024
9	18-Feb-2023	33	08-Mar-2024
10	06-Mar-2023	34	24-Mar-2024
11	22-Mar-2023	35	09-Apr-2024
12	07-Apr-2023	36	25-Apr-2024
13	23-Apr-2023	37	11-May-2024
14	09-May-2023	38	27-May-2024
15	25-May-2023	39	12-Jun-2024
16	10-Jun-2023	40	28-Jun-2024
17	26-Jun-2023	41	14-Jul-2024
18	12-Jul-2023	42	30-Jul-2024
19	28-Jul-2023	43	15-Aug-2024
20	13-Aug-2023	44	31-Aug-2024
21	29-Aug-2023	45	16-Sep-2024
22	14-Sep-2023	46	02-Oct-2024
23	30-Sep-2023	47	18-Oct-2024
24	16-Oct-2023	48	03-Nov-2024

10. REFERENCES

- Azetsu-Scott, K., A. Clarke, K. Falkner, J. Hamilton, E. P. Jones, C. Lee, B. Petrie, S. Prinsenberg, M. Starr, and P. Yeats (2010). Calcium carbonate saturation states in the waters of the Canadian Arctic Archipelago and the Labrador Sea. *J. Geophys. Res.* 115, C11021, doi:10.1029/2009JC005917.
- Azetsu-Scott, K., B. Petrie, P. Yeats and C. Lee (2012), Composition and fluxes of freshwater through Davis Strait using multiple chemical tracers. *J. Geophys. Res.* 117, C12011, 10.1029/2012/JC008172.
- Balazy, K., Trudnowska, E., Wichorowski, M., Błachowiak-Samołyk, K. (2018). Large versus small zooplankton in relation to temperature in the Arctic shelf region. *Polar Res.* 37: 1.
- Brown, P. J., and D. Rayner (2015). Standard operating procedure for the pre-deployment setup of the McLane Remote Access Sampler (RAS) Rep., National Oceanography Centre, Southampton, UK.
- Carmack, E.C., et al., (2016). Freshwater and its role in the Arctic Marine System: Sources, disposition, storage, export, and physical and biogeochemical consequences in the Arctic and global oceans, *J. Geophys. Res. Biogeosci.* 121, 675-717, doi:10.1002/2015JG003140.
- Casacuberta, N., Castrillejo, M., Wefing, A.-M., Bollhalder, S., Kündig, K., Synal, H.-A., and Wacker, L. (2020). Rapid and high precision C-14 analysis in small DIC seawater samples and its future application as an ocean tracer, EGU General Assembly 2020, Online, 4–8 May 2020, EGU2020-3581, <https://doi.org/10.5194/egusphere-egu2020-3581>
- Castrillejo et al., (2017). Anthropogenic ²³⁶U and ¹²⁹I in the Mediterranean Sea: First comprehensive distribution and constrain of their sources. *Sci. Total. Environ.* 593, 745-759.
- Dickson, A.G., Sabine, C.L. and Christian, J.R., Eds. (2007). *Guide to Best Practices for Ocean CO₂ Measurements*. PICES Special Publication 3, 191 pp.
- GEOTRACES Cookbook (2017). *Sampling and Sample-handling Protocols for GEOTRACES Cruises* (Cookbook, version 3.0, 2017) <https://www.geotraces.org/methods-cookbook/>
- Gjerdrum, C., D.A. Fifield, and S.I. Wilhelm (2012). *Eastern Canada Seabirds at Sea (ECSAS) Standardized Protocol for Pelagic Seabird Surveys from Moving and Stationary Platforms*. Canadian Wildlife Service Technical Report Series No. 515. Atlantic Region. vi + 36 pp.

- Gladish, C., D. Holland and C. Lee (2015). Ocean Boundary Conditions for Jakobshavn Glacier: Part II. Provenance and Sources of Variability of Disko Bay and Ilulissat Icefjord Waters, 1990-2011. *J. Phys. Ocean.* 45, 33-63, doi:10.1175/JPO-D-14-0045.1.
- Green, E.P., Dagg, M.J. (1997). Mesozooplankton associations with medium to large marine snow aggregates in the northern Gulf of Mexico. *J. Plankton Res.* 19: 435-447.
- Haine, T.W.M., B. Curry, R. Gerdes, E. Hansen, M. Karcher, C. Lee, B. Rudels, G. Spreen, L. deSteur, K.D. Stewart and R. Woodgate (2015). Arctic freshwater export: Status, mechanisms and prospects. *Global Planetary Change*, 125, 13-35, doi:10.1016/j.gloplacha.2014.11.013.
- Hammill, E., E. Johnson, T.B. Atwood, J. Harianto, C. Hinchliffe, P. Calosi, and M. Byrne (2017). Ocean acidification alters zooplankton communities and increases top-down pressure of a cubozoan predator. *Global Change Biology*, 24, e128-e138.
- Hátún, H., Payne, M.R., Beaugrand, G., Reid, P.C., Sando, A.B., Drange, H., Hansen, B., Jacobsen, J.A., Bloch, D. (2009). Large bio-geographical shifts in the north-eastern Atlantic Ocean: From the subpolar gyre, via plankton, to blue whiting and pilot whales. *Prog. Oceanogr.* 80, 149-162.
- Hátún, H., Azetsu-Scott, K., Somavilla, R. et al. (2017). The subpolar gyre regulates silicate concentrations in the North Atlantic. *Sci. Rep.* 7, 14576, doi:10.1038/s41598-017-14837-4
- Holland, D.M., Thomas, R.H., de Young, B., Ribergaard, M.H., and Lyberth, B. (2008). Acceleration of Jakobshavn Isbr. triggered by warm subsurface ocean waters. *Nat. Geosci.* 1, 659–664.
- Jahn, A., and M.M. Holland (2013). Implications of Arctic sea ice changes for North Atlantic deep convection and the meridional overturning circulation in CCSM5-CMIP5 simulations, *Geophys. Res. Lett.* 40, 1206-1211, doi:10.1002/grl50183.
- Johnson, K.M., A.E. King, and M. Mc Sieburth (1985). Coulometric TCO. analyses for marine studies: An introduction, *Mar. Chem.* 16, 61–82.
- Karcher, M., Gerdes, R., Kauker, f., Kaberle, C. and Yashayaev, I. (2005). Arctic Ocean change heralds North Atlantic freshening. *Geophys. Res. Lett.* L21606, doi:10.1029/2005GL023861.
- Kawano, T. (2010). Method for salinity (conductivity ratio) measurement. In: *The GO-SHIP Repeat Hydrography Manual: A Collection of Expert Reports and Guidelines, Version 1*, Hood, E.M., C.L. Sabine, and B.M. Sloyan, eds. IOCCP Report 14; ICPO Publication Series 134, 13 pp., doi: 10.25607/OBP-1339

- Koski, M., Valencia, B., Newstead, R., Thiele, C. (2020). The missing piece of the upper mesopelagic carbon budget? Biomass, vertical distribution and feeding of aggregate-associated copepods at the PAP site, *Prog. Oceanogr.* 181, 102243.
- Langdon, C. (2010). Determination of dissolved oxygen in seawater by Winkler titration using amperometric technique. In: *The GO-SHIP Repeat Hydrography Manual: A Collection of Expert Reports and Guidelines. Version 1*. Hood, E.M., C.L. Sabine, and B.M. Sloyan, eds. IOCCP Report Number 14; ICPO Publication Series Number 134, 18 pp., doi: <https://doi.org/10.25607/OBP-1350>
- Myers, P.G., and Ribergaard, M.H. (2013). Warming of the polar water layer in Disko Bay and potential impact on Jakobshavn Isbrae, *J. Phys. Oceanogr.* 43(12), 2629-2640.
- Paffrath, R., Laukert, G., Bauch, D., Rutgers van der Loeff, M., and Pahnke, K. (2021). Separating individual contributions of major Siberian rivers in the Transpolar Drift of the Arctic Ocean, *Sci. Rep.* 11, doi: 10.1038/s41598-021-86948-y
- Prowse, T., A. Bring, J. Mård, and E. Carmack (2015). Arctic Freshwater Synthesis: Introduction, *J. Geophys. Res. Biogeosci.* 120, 2121-2131, doi:10.1002/2015JG003127.
- Schuster, U., and A.J. Watson (2007). A variable and decreasing sink for atmospheric CO₂ in the North Atlantic, *J. Geophys. Res.* 112, C11006, doi:10.1029/2006JC003941.
- Serreze, M.C., Barrett, A.P., Slater, A.G., Woodgate, R.A., Aagard, K., Lammers, R., Steele, M., Moritz, R., Meredith, M., Lee, C.M. (2006). The large-scale freshwater cycle of the Arctic, *J. Geophys. Res.* 111, C11010, doi:10.1029/2005JC003424.
- Straneo, F., and P. Heimbach (2013). North Atlantic warming and the retreat of Greenland's outlet glaciers, *Nature* 504, 36–43.
- Yang, Q., Dixon, T., Myers, P. et al. (2016). Recent increases in Arctic freshwater flux affects Labrador Sea convection and Atlantic overturning circulation. *Nat. Commun.* 7, 10525.

11. APPENDIX: CRUISE NARRATIVE

Time in local (UTC-2) unless otherwise noted.

27–28 September

Mobilization.

COVID

The roommate of one Nuuk-based science team member has been exhibiting symptoms and has tested positive for COVID. This creates a complication in terms of whether the science team member should be allowed to sail. The solution is to have the person tested and if negative, to quarantine for 5 days with meals delivered by only one person to limit exposure. If a PCR test is negative then masking for an additional 5 days.

29 September

Finish mobilization. The combination of an expanded science team, the need to maintain flexibility to create a COVID isolation room and the limited science berthing of the Ocean Class vessels has left some teams short-handed. We'll need to evaluate the impact as the cruise progresses, but one mitigation might be to bring additional personnel to assist with setup.

COVID: Science and crew all test negative (PCR) clearing them to sail.

30 September

Depart Nuuk at 10:00. Fairly calm, but winds and sea build over the evening. Transit to WG-1, planning to sweep east to recover the Greenland shelf moorings during the day on 1 Oct, then move westward along the line occupying the CTD stations at night.

1 October

Slow to 7 kts overnight, arriving at WG1/ML13 at roughly 10:00. Winds 30 kts and sea state too rough to safely conduct the initial mooring recoveries.

Elect to instead begin CTD sampling, working westward starting with station ML13 (at the WG-1 site). Sample ML13 and ML12, sorting out procedures and training watchstanders. Weather deteriorates through the evening, with 30 kt winds and waves reaching 3.3 m. CTD trolley breaks down at ML12, so that ML11 sampling take place on

deck rather than in the hanger. Soon after midnight, conditions deteriorate to the point that sampling is deemed unsafe and we halt CTD operations. ML11 sampling hindered by waves breaking on deck, dousing the samplers and resulting in the loss of some sampling bottles.

COVID: A member of the science team shows COVID symptoms, with antigen and PCR tests both positive. Isolate the person in the ADA stateroom and antigen test entire science team. Although all are negative, the two people who share a room and/or head with the infected individual will mask for the next 5 days and take meals in their room.

2 October

Winds and waves remain strong through the morning. R/V *Armstrong* maintains station at ML10 as we wait for conditions to improve enough to resume CTD sampling.

Emily manages to repair the CTD sled motor, making it possible to shift the CTD to the hanger for sampling.

Conditions improve enough to restart CTD operations at 13:00, beginning with ML10. Deployment and sampling go smoothly. Winds and sea state decrease through the afternoon. Anticipate beginning mooring operations at first light on 3 October with the recovery of C3.

3 October

Complete ML13 – ML07 CTDs over night, but without nets due to sea state. Arrive at C3 around 05:00 and hold for daylight to start mooring operations.

Mooring recoveries proceed quickly with minimal winds and low sea state. Begin C3 recovery at first light, releasing at roughly 07:30L. On surface at 07:56Z with all gear on deck at 09:24L. C2 recovery begins at 12:00L, with all gear aboard at 13:12L. C2 IceCAT top missing. C1 recovery begins at 15:22L, with all gear aboard by 16:00L.

BI2 and BI4 deck sheets mislabeled (swapped), but error is discovered and corrected. BI4 recovery begins at 17:11L with all gear on deck at 17:26L. IceCAT top recovered. BI2 recovery at 18:00L. IceCAT top recovered.

Begin CTD and net sampling at ML01, working east. Sampling begins at 18:00.

4 October

ML01–ML05 sampled overnight. Continue working eastward, sampling ML06. Skip ML08 to reach C4 with enough daylight to allow recovery. Recover C4 (IceCAT top lost), which pops a few hundred meters (rough guess) from where it was expected.

IceCAT is missing. On recovery we find that the line between the syntactic sphere and the ADCP cage has been badly abraded in multiple places. This, together with the apparent displacement, suggest that the mooring was caught and dragged at some time during its two-year deployment.

With C4 on deck, return to ML08 to conduct net casts. Multinet sent deep (much deeper than trigger depth) in attempt to force it to trip. It again returns to deck without firing. Current thinking is that this may be an issue with the pressure sensor,

Continue working east, sampling ML stations with CTD and nets. Plan is to arrive at C5 by 06:00 tomorrow.

5 October

Starting with C5, work eastward recovering C5 (IceCAT top recovered), C6 (IceCAT top lost), WG1, WG1.5 (IceCAT top recovered), WG2 (IceCAT top lost) and WG4 (IceCAT top recovered) over the course of a long day.

Evening spent finishing eastern half of Mooring Line CTD stations.

6 October

Transit to NL25, at the eastern end of the Northern Line and begin occupying stations working east to west.

7 October

Sample NL12, immediately before the apex of the Northern Line, very early morning. Following the station, break off to transit north to the BPR site.

8 October

Transit to BPR mooring site for recovery and CTD station. Glassy calm weather.

9 October

Arrive at BPR site before breakfast. Attempt to enable the release at ranges of 100–500 m from the anchor site, to the north and south, but release fails to respond. Sending release commands also fails to release the mooring. We decide to drag despite the fact that the BPR mooring is an exceptionally poor target, standing only 6–7 m off the bottom. Conduct the first of two CTD casts prior to dragging, with the chemistry and

biology teams arguing to lead with the deep cast. Dragging begins around lunchtime and extends until dark. Three attempts fail to catch the mooring. Dragging gear aboard at 21:00, followed by shallow CTD cast, ring and bongo nets.

The loss of the 2020–2022 BPR means that there is no timeseries and this 2020 site, which clearances forced to be ~45 nm NNE of the target BPR site. Because the target site will save half a day of transit for future service cruises, we elect to relocate the BPR mooring back to the originally planned location.

10 October

Transit from BPR-2020 to BPR and deploy the mooring.

11 October

NL line CTDs and nets. Bodil finds a fix for the multinet and is able to begin sampling.

12 October

Finish NL stations early morning and transit to BI2. Begin mooring deployments immediately after lunch.

Shift C1 back to original position, onto the mooring line, from the more southern site it had migrated to for the past few deployments. This required the addition of a 20-m adjustment shot to correct for bottom depth.

Halt operations due to weather, as nighttime brings 40 kt winds and higher sea state. Multinet is damaged on a cast at C1 as conditions worsen to the point where we decide to cancel the rest of the night's mooring deployments. We will re-evaluate in the morning.

13 October

Sea state improves steadily through the morning, allowing a late morning start for mooring operations. With transits, this allows time to deploy three mid-strait moorings, C2, C3, and C4, before switching to net tows, working to collect multinet stations that were unsuccessful or bypassed earlier in the cruise due to instrument malfunctions.

14 October

Begin mooring operations early, finishing C5 before breakfast. Deploy C5, C6, WG1, WG1.5, WG2, and WG4 to complete the array. Conduct mooring line multinet sampling that was skipped earlier due to issues with getting the multinet to fire properly. Enough time remains to sample the set of three Labrador Sea lines, but long-term forecasts predict severe weather over the west Greenland shelf in the final days of the cruise. Predicted sea states could pose a barrier between the interior strait and Nuuk fjord, blocking access to the port for a couple of days around our scheduled return. To maintain better control of time, we chose to work the Labrador Sea lines west to east. Begin transit from the east end of the mooring line to the western end of the LSW line in the evening.

15 October

Transit to the LSW line, arriving late at night to begin sampling.

16 October

Sample the LSW line.

17 October

Finish the LSW line. Multiple models predict severe winds and sea state (>40 kts, 6–7 m seas) over the West Greenland shelf, beginning late on 20 Oct and extending to the morning of 22 Oct. Predicted conditions would make transit across the shelf difficult – slow at best and perhaps impossible. Sampling the LSC line would place us offshore when the system passes through, forcing a difficult transit or a delayed return. To avoid this, we will bypass the LSC line, sampling LSE and then working in the shelter of the fjords surrounding Nuuk during the period of high winds and sea state. We will target two lines regularly sampled by GINR researchers, using the capabilities of the Davis Strait team to expand the suite of parameters. This has the advantage of keeping the ship out of 6 m seas, greatly increasing the likelihood of returning to port on time.

18 October

Sample the LSE line.

19 October

Wrap up sampling on the LSE line. Shift slightly northwest to begin the GINR Gothåbsfjord (GF) line with a series of stations that cross the shelf that leads into the fjord system. Weather remains good through the day.

20 October

After sampling the outer stations of the GINR Gothåbsfjord line, we shelter from the oncoming weather behind an island near Nuuk, waiting for daylight before moving further into the fjord. Wake to strong winds gusting to 40+ kts, and whitecaps even in the shelter of the outer fjord. The predicted weather system has arrived. R/V *Armstrong* encounters little ice as it moves northeast through the fjord. Initially, we sample stations as we come to them, but then decide to run as far into the fjord as ice will allow before reversing to sample the stations on the way out. Resources are running short, and this allows us to focus the remaining sample bottles on the high-priority stations nearer to the ice, and to better control our time,

21 October

Shelter offshore of Nuuk overnight as winds build to 40+ kts. Occupy a section along the thalweg of Ameralik Fjord, running into the fjord to GINR station AM11, stopping one station short of the end due to uncertainty about water depth. Despite severe winds and high waves over the shelf, conditions are very calm within the fjord. The section shows sharp differences between this and Gothåbsfjord, with its marine terminating glacier. Near-surface $p\text{CO}_2$ is elevated within Ameralik Fjord, in contrast to low values observed in Gothåbsfjord the day before.

12. APPENDIX: LIST OF CRUISE PARTICIPANTS

Name	Institution	Role
Craig Lee	Applied Physics Lab, Univ. of Washington (USA)	Chief Scientist
Eric Boget	Applied Physics Lab, Univ. of Washington (USA)	Engineer
Jed Lenetsky	University of Colorado Boulder (USA)	Grad Student
Kate Stafford	Oregon State University (USA)	PI
Angela Szesciorka	Oregon State University (USA)	Postdoc
Kumiko Azetsu-Scott	Bedford Institute of Oceanography (Canada)	PI
Carrie-Ellen Gabriel	Bedford Institute of Oceanography (Canada)	Scientist
Maddison Proudfoot	Bedford Institute of Oceanography (Canada)	Scientist
Thomas Juul Pedersen	Greenland Institute of Natural Resources and Greenland Climate Center (Greenland)	Scientist
Else Ostermann	Greenland Institute of Natural Resources and Greenland Climate Center (Greenland)	Lab Technician
Tobias Vonnahme	Greenland Institute of Natural Resources and Greenland Climate Center (Greenland)	Postdoc
Hannah Felicitas Kuhn	Greenland Institute of Natural Resources and Greenland Climate Center (Greenland)	Grad Student
Caroline Gjelstrup	Danish Technical University (Denmark)	Grad Student
Bodil Toftegård	Danish Technical University (Denmark)	Grad Student
Pete Brown	National Oceanography Centre, Southampton (UK)	Scientist
Alice Marzocchi	National Oceanography Centre, Southampton (UK)	Scientist
Lisa Gerlinde Thekla Leist	Swiss Federal Inst of Technology, Zurich (Switzerland)	Grad Student
Victoria Silverman	Louisiana Universities Marine Consortium (USA)	Undergrad
Holly Hogan	Canadian Wildlife Service/bird observer (Canada)	Scientist
Siobhan McDonald		Artist

13. APPENDIX: CODE OF CONDUCT

Seagoing science relies on diverse groups of researchers and crew members to carry out complex operations in an often-challenging environment. Interactions and relationships between individuals define the character of a seagoing team, and thus take on great importance. Teamwork is paramount to success, and supportive, collegial teams tend to be highly effective. Seagoing expeditions place unique demands on individuals, confining them to work and live in close proximity for extended periods of time, blurring the lines between work and personal spaces. Stresses associated with executing complex tasks and difficult environmental conditions can amplify these challenges.

As a community, we are all responsible for maintaining a culture of professionalism and respect. During the expedition, the shipboard environment is both professional workspace and personal habitat, and the boundaries between work and personal time are often blurred. We aim to provide a safe and inclusive working environment for all cruise participants by grounding the culture in civility and respect.

Expected Conduct

- Be fair, respectful, and supportive of others.
- Be welcoming and inclusive of all people.
- Act ethically and with integrity.
- Be respectful of the ship and crew. The science team are visitors aboard the ship, which the crew considers home.
- Provide positive feedback and constructive criticism.
- Be open to receiving and acting on constructive criticism.

Unacceptable Behavior

- Sexual harassment. Sexual harassment is a specific form of harassment that includes unwelcome sexual advances or contact, gender stereotyping, pressure for sexual favors, relationship violence, date rape, non-consensual intercourse, and sexual assault.
- Any form of harassment, sexual or otherwise, or retaliation against any individual who brought a complaint of harassment.
- Bullying.
- Discrimination based on age, gender, gender identity, sexual orientation, shipboard role.
- Possession of use of illegal drugs or alcohol.

Resources

Should you need to talk with someone or report suspected or alleged misconduct, please reach out to any or all the following knowing that we will take any complaint seriously and assist in finding a resolution. All reports will be treated as confidential.

- Craig Lee (chief scientist): craiglee@uw.edu
- Kent Sheasley (Captain, R/V *Armstrong*): master@armstrong.who.edu
- Kate Stafford: kate.stafford@oregonstate.edu
- Kumiko Azetsu-Scott: Kumiko.Azetsu-Scott@dfo-mpo.gc.ca
- Your supervisor
- EEO or Title IX Officer at your institution
- WHOI EEO Officer: eeo@who.edu, 508-289-2705
- WHOI Title IX Coordinator: titleix@who.edu, 508-289-2848